Analysis Procedures for Evaluating Superheavy Load Movement on Flexible Pavements, Volume IX: Appendix H, Analysis of Cost Allocation Associated With Pavement Damage Under a Superheavy Load Vehicle Movement

PUBLICATION NO. FHWA-HRT-18-057

DECEMBER 2018

U.S. Department of Transportation
Federal Highway Administration

Research, Development, and Technology
Turner-Fairbank Highway Research Center
6300 Georgetown Pike
McLean, VA 22101-2296

FOREWORD

The movement of superheavy loads (SHLs) on the Nation's highways is an increasingly common, vital economic necessity for many important industries, such as chemical, oil, electrical, and defense. Many superheavy components are extremely large and heavy (gross vehicle weights in excess of a few million pounds), and they often require specialized trailers and hauling units. At times, SHL vehicles have been assembled to suit the load being transported, and therefore, the axle configurations have not been standard or consistent. Accommodating SHL movements without undue damage to highway infrastructure requires the determination of whether the pavement is structurally adequate to sustain the SHL movement and protect any underground utilities. Such determination involves analyzing the likelihood of instantaneous or rapid load-induced shear failure of the pavement structure.

The goal of this project was to develop a comprehensive analysis process for evaluating SHL movement on flexible pavements. As part of this project, a comprehensive mechanistic-based analysis approach consisting of several analysis procedures was developed for flexible pavement structures and documented in a 10-volume series of Federal Highway Administration reports—a final report and 9 appendices.[1–9] This is *Analysis Procedures for Evaluating Superheavy Load Movement on Flexible Pavements, Volume IX: Appendix H, Analysis of Cost Allocation Associated With Pavement Damage Under a Superheavy Load Vehicle Movement*, and it details the methodology of allocating the cost of likely damage associated with an SHL-vehicle movement on flexible pavements. This report is intended for use by highway agency pavement engineers responsible for assessing the structural adequacy of pavements in the proposed route and identifying mitigation strategies, where warranted, in support of the agency's response to SHL-movement permit requests.

Cheryl Allen Richter, Ph.D., P.E.
Director, Office of Infrastructure
Research and Development

TECHNICAL REPORT DOCUMENTATION PAGE

1. Report No. FHWA-HRT-18-057	2. Government Accession No.	3. Recipient's Catalog No.
4. Title and Subtitle Analysis Procedures for Evaluating Superheavy Load Movement on Flexible Pavements, Volume IX: Appendix H, Analysis of Cost Allocation Associated With Pavement Damage Under a Superheavy Load Vehicle Movement		5. Report Date December 2018 6. Performing Organization Code
7. Author(s) Dario D. Batioja-Alvarez (0000-0002-1094-553X), Elie Y. Hajj (ORCID: 0000-0001-8568-6360), and Raj V. Siddharthan (ORCID: 0000-0002-3847-7934)		8. Performing Organization Report No. WRSC-UNR-201710-01H
9. Performing Organization Name and Address Department of Civil and Environmental Engineering University of Nevada 1664 North Virginia Street Reno, NV 89557		10. Work Unit No. 11. Contract or Grant No. DTFH61-13-C-00014
12. Sponsoring Agency Name and Address Office of Infrastructure Research and Development Federal Highway Administration Turner-Fairbank Highway Research Center 6300 Georgetown Pike McLean, VA 22101		13. Type of Report and Period Covered Final Report; August 2013–July 2018 14. Sponsoring Agency Code HRDI-20
15. Supplementary Notes Nadarajah Sivaneswaran (HRDI-20; ORCID: 0000-0003-0287-664X), Office of Infrastructure Research and Development, Turner-Fairbank Highway Research Center, served as the Contracting Officer's Representative.		

16. Abstract

The movement of superheavy loads (SHLs) has become more common over the years, since it is a vital necessity for many important industries, such as chemical, oil, electrical, and defense. SHL hauling units are much larger in size and weight compared to standard trucks. SHL gross vehicle weights may be in excess of a few million pounds, so they often require specialized trailers and components with nonstandard spacing between tires and axles. Accommodating SHL movements requires the determination of whether the pavement is structurally adequate and involves the analysis of the likelihood of instantaneous or rapid load-induced shear failure. As part of the Federal Highway Administration project, Analysis Procedures for Evaluating Superheavy Load Movement on Flexible Pavements, a mechanistic–empirical based approach that relied on the use of locally calibrated performance models was proposed for the analysis of cost allocation associated with pavement damage under an SHL-vehicle movement. The approach considered many governing factors and provided useful ways to assess pavement damage from a single pass of an SHL vehicle. The approach was based on the determination of critical pavement responses associated with important pavement distress modes. A parametric analysis was conducted, and it was found that several factors can influence the calculation of pavement damage–associated costs (PDACs). For instance, PDACs are highly impacted by pavement temperature, SHL-vehicle operating speed, rehabilitation distress threshold, and variation in pavement structure. On the other hand, the annual daily truck traffic and the selection of the reference vehicle were found to be minimally influential in the cost allocation analysis.

17. Key Words Superheavy load, pavement damage, cost allocation, flexible pavement, vehicle miles traveled	18. Distribution Statement No restrictions. This document is available to the public through the National Technical Information Service, Springfield, VA 22161. http://www.ntis.gov		
19. Security Classif. (of this report) Unclassified	20. Security Classif. (of this page) Unclassified	21. No. of Pages 52	22. Price N/A

Form DOT F 1700.7 (8-72) Reproduction of completed page authorized.

SI* (MODERN METRIC) CONVERSION FACTORS

APPROXIMATE CONVERSIONS TO SI UNITS

Symbol	When You Know	Multiply By	To Find	Symbol
		LENGTH		
in	inches	25.4	millimeters	mm
ft	feet	0.305	meters	m
yd	yards	0.914	meters	m
mi	miles	1.61	kilometers	km
		AREA		
in^2	square inches	645.2	square millimeters	mm^2
ft^2	square feet	0.093	square meters	m^2
yd^2	square yard	0.836	square meters	m^2
ac	acres	0.405	hectares	ha
mi^2	square miles	2.59	square kilometers	km^2
		VOLUME		
fl oz	fluid ounces	29.57	milliliters	mL
gal	gallons	3.785	liters	L
ft^3	cubic feet	0.028	cubic meters	m^3
yd^3	cubic yards	0.765	cubic meters	m^3
		NOTE: volumes greater than 1000 L shall be shown in m^3		
		MASS		
oz	ounces	28.35	grams	g
lb	pounds	0.454	kilograms	kg
T	short tons (2000 lb)	0.907	megagrams (or "metric ton")	Mg (or "t")
		TEMPERATURE (exact degrees)		
^oF	Fahrenheit	5 (F-32)/9 or (F-32)/1.8	Celsius	^oC
		ILLUMINATION		
fc	foot-candles	10.76	lux	lx
fl	foot-Lamberts	3.426	$candela/m^2$	cd/m^2
		FORCE and PRESSURE or STRESS		
lbf	poundforce	4.45	newtons	N
lbf/in^2	poundforce per square inch	6.89	kilopascals	kPa

APPROXIMATE CONVERSIONS FROM SI UNITS

Symbol	When You Know	Multiply By	To Find	Symbol
		LENGTH		
mm	millimeters	0.039	inches	in
m	meters	3.28	feet	ft
m	meters	1.09	yards	yd
km	kilometers	0.621	miles	mi
		AREA		
mm^2	square millimeters	0.0016	square inches	in^2
m^2	square meters	10.764	square feet	ft^2
m^2	square meters	1.195	square yards	yd^2
ha	hectares	2.47	acres	ac
km^2	square kilometers	0.386	square miles	mi^2
		VOLUME		
mL	milliliters	0.034	fluid ounces	fl oz
L	liters	0.264	gallons	gal
m^3	cubic meters	35.314	cubic feet	ft^3
m^3	cubic meters	1.307	cubic yards	yd^3
		MASS		
g	grams	0.035	ounces	oz
kg	kilograms	2.202	pounds	lb
Mg (or "t")	megagrams (or "metric ton")	1.103	short tons (2000 lb)	T
		TEMPERATURE (exact degrees)		
^oC	Celsius	1.8C+32	Fahrenheit	^oF
		ILLUMINATION		
lx	lux	0.0929	foot-candles	fc
cd/m^2	$candela/m^2$	0.2919	foot-Lamberts	fl
		FORCE and PRESSURE or STRESS		
N	newtons	0.225	poundforce	lbf
kPa	kilopascals	0.145	poundforce per square inch	lbf/in^2

ANALYSIS PROCEDURES FOR EVALUATING SUPERHEAVY LOAD MOVEMENT ON FLEXIBLE PAVEMENTS PROJECT REPORT SERIES

This volume is the ninth of 10 volumes in this research report series. Volume I is the final report, and Volume II through Volume X consist of Appendix A through Appendix I. Any reference to a volume in this series will be referenced in the text as "Volume II: Appendix A," "Volume III: Appendix B," and so forth. The following list contains the volumes:

Volume	Title	Report Number
I	Analysis Procedures for Evaluating Superheavy Load Movement on Flexible Pavements, Volume I: Final Report	FHWA-HRT-18-049
II	Analysis Procedures for Evaluating Superheavy Load Movement on Flexible Pavements, Volume II: Appendix A, Experimental Program	FHWA-HRT-18-050
III	Analysis Procedures for Evaluating Superheavy Load Movement on Flexible Pavements, Volume III: Appendix B, Superheavy Load Configurations and Nucleus of Analysis Vehicle	FHWA-HRT-18-051
IV	Analysis Procedures for Evaluating Superheavy Load Movement on Flexible Pavements, Volume IV: Appendix C, Material Characterization for Superheavy Load Movement Analysis	FHWA-HRT-18-052
V	Analysis Procedures for Evaluating Superheavy Load Movement on Flexible Pavements, Volume V: Appendix D, Estimation of Subgrade Shear Strength Parameters Using Falling Weight Deflectometer	FHWA-HRT-18-053
VI	Analysis Procedures for Evaluating Superheavy Load Movement on Flexible Pavements, Volume VI: Appendix E, Ultimate and Service Limit Analyses	FHWA-HRT-18-054
VII	Analysis Procedures for Evaluating Superheavy Load Movement on Flexible Pavements, Volume VII: Appendix F, Failure Analysis of Sloped Pavement Shoulders	FHWA-HRT-18-055
VIII	Analysis Procedures for Evaluating Superheavy Load Movement on Flexible Pavements, Volume VIII: Appendix G, Risk Analysis of Buried Utilities Under Superheavy Load Vehicle Movements	FHWA-HRT-18-056
IX	Analysis Procedures for Evaluating Superheavy Load Movement on Flexible Pavements, Volume IX: Appendix H, Analysis of Cost Allocation Associated With Pavement Damage Under a Superheavy Load Vehicle Movement	FHWA-HRT-18-057
X	Analysis Procedures for Evaluating Superheavy Load Movement on Flexible Pavements, Volume X: Appendix I, Analysis Package for Superheavy Load Vehicle Movement on Flexible Pavement (SuperPACK)	FHWA-HRT-18-058

TABLE OF CONTENTS

LIST OF FIGURES

LIST OF TABLES

LIST OF ABBREVIATIONS AND SYMBOLS

Abbreviations

AADTT	average annual daily truck traffic
AASHTO	American Association of State Highway and Transportation Officials
AC	asphalt concrete
CAB	crushed aggregate base
ESAL	equivalent single-axle load
FHWA	Federal Highway Administration
GVW	gross vehicle weight
LR	life reduction
ME	mechanistic–empirical
MEPDG	*Mechanistic–Empirical Pavement Design Guide*
NAPCOM	National Pavement-Cost Model
OW	overweight
PaveDAT	Pavement Damage Analysis Tool
PDAC	pavement damage–associated cost
PWV	present worth value
RSL	remaining service life
SG	subgrade
SHA	State highway agency
SHL	superheavy load
VMT	vehicle miles traveled

Symbols

Cost	pavement-repair cost in dollars per lane-mile
Discount Rate	real discount rate that reflects the time value of money with no inflation premium (should be used in conjunction with noninflated-dollar cost estimates of future investments)
d_{Nstd}	distress after specific number of vehicle passes
$d_{Nstd:10,000}$	distress after 10,000 vehicle passes
$d_{truck:eq+1}$	damage caused by an extra pass of superheavy vehicles after $N_{truck:eq}$
E_{AC}	asphalt concrete layer dynamic modulus
GWT	depth of ground water table
h_s	thickness of unbound material layer
k_{f1}	fatigue cracking calibration factor
k_{f2}	fatigue cracking calibration factor for tensile strain exponent
k_{f3}	fatigue cracking calibration factor for stiffness exponent
k_{r1}	asphalt concrete permanent deformation calibration factor
k_{r2}	asphalt concrete permanent deformation calibration factor for temperature exponent
k_{r3}	asphalt concrete permanent deformation calibration factor for number of load repetitions exponent
k_{s1}	unbound materials calibration factor

LR	life reduction
M_R	resilient modulus of the unbound layer
N	number of axle group repetitions
n	pavement service life in years
N_f	number of load applications to fatigue cracking failure
$N_{failure}$	estimated number of passes of superheavy load or reference vehicles to the threshold failure
$N_{i:failure}$	estimated number of passes to the same threshold failure for the individual axle groups within the superheavy load or reference vehicle
N_r	number of load applications to asphalt concrete permanent deformation failure
$N_{std:f}$	predicted number of reference-vehicle passes to failure
$N_{truck:eq}$	number of superheavy vehicle passes to cause same distress as d_{Nstd}
PWV	present worth value
RSL	remaining service life
T	temperature at the middepth of the asphalt concrete layer
W_c	water content
Year of Last Repair	year when last structural pavement repair took place
Year of Next Repair	year of the next scheduled structural pavement repair
Year of SHL Pass	year when superheavy load movement is expected to take place
β	power parameter for material property
β_{f1}	fatigue cracking laboratory calibration factor
β_{f2}	fatigue cracking laboratory calibration factor for tensile exponent
β_{f3}	fatigue cracking laboratory calibration factor for stiffness exponent
β_{r1}	asphalt concrete permanent deformation local calibration factor
β_{r2}	asphalt concrete permanent deformation local calibration factor for temperature exponent
β_{r3}	asphalt concrete permanent deformation local calibration factor for number of load repetitions exponent
β_{s1}	unbound materials local calibration factor
$\Delta N_{std:eq}$	additional passes of the equivalent reference vehicle to cause $d_{truck:eq+1}$
$\delta(N)$	permanent deformation corresponding to N-load for unbound materials
ε_o	intercept determined from laboratory repeated load permanent deformation tests
ε_p	plastic strain at the middepth of the asphalt concrete layer
ε_r	resilient strain at the middepth of the asphalt concrete layer
ε_t	maximum tensile strain at bottom of asphalt concrete layer
ε_v	vertical resilient strain computed from layer in question
ρ	material property parameter

CHAPTER 1. INTRODUCTION

Generally, loadings from movement of superheavy load (SHL) vehicles are not accounted for in structural designs of highway pavements. SHL vehicles may involve gross vehicle weights (GVWs) in excess of a few million pounds, often requiring specialized trailers and components with nonstandard spacing between tires and axles. Thus, the assignment of highway cost responsibilities due to pavement damage associated with passes of SHL vehicles is a significant task that needs to be addressed. The operation of large and heavy vehicles can lead to a speedy deterioration of the roadway system, necessitating additional resources to maintain acceptable conditions of the roadway pavements. As part of this study, Analysis Procedures for Evaluating Superheavy Load Movement on Flexible Pavements, a cost allocation methodology is recommended to determine the extent of pavement damage and associated costs from SHL-vehicle movements on flexible pavements. The quantification of increased costs due to repair and maintenance activities attributable to SHL-vehicle movement is helpful to engineers and practitioners so that informed decisions on the issuance of SHL permits can be made.

State highway agencies (SHAs) issue special permits for SHL-vehicle movements and collect a nominal fee, making the operation of such vehicles legal on the State's highway network. However, quantifying pavement damage attributed to an SHL movement is a challenging task. An array of factors specific to each SHL movement (axle and tire loadings and configurations, traveling speed, temperature and properties of existing pavement layers at the time of the movement, etc.) influences the magnitude of the load-induced pavement damage. SHL vehicles generally have nonstandard axle configurations, and any additional pavement damage caused by their operation is generally not considered in the new and rehabilitation designs of pavements. Since the heavier axle loads of SHL vehicles can introduce greater stresses and strains in the pavement compared to those estimated under a traditional truck loading, a single SHL-vehicle pass could induce the same damage as multiple passes of a standard heavy vehicle (herein referred to as a reference vehicle), leading to a faster deterioration in the pavement condition than anticipated. The rate of deterioration is highly influenced by the structural capacity of the existing pavement as well as the climatic conditions at the time of the SHL movement.

Another challenge associated with determining pavement damage due to an SHL movement is properly accounting for the characteristics of the existing pavement layers at the time of the movement. For instance, the viscoelastic property of the asphalt concrete (AC) layer is critical as it influences the load-induced pavement responses with the SHL movements often being at much lower speeds. For example, pavement damage caused by an SHL vehicle operating during the summer may be significantly different than the damage caused by the same vehicle operating during a different season, or an SHL vehicle operating during daytime hours versus during nighttime hours of the same day.

Engineers and transportation officials need convincing and reliable tools to evaluate and understand pavement damage as well as the associated costs due to SHL vehicles operating under different loading and environmental conditions. It should be noted that the analysis of cost allocation associated with pavement damage under an SHL-vehicle movement should only be considered after ruling out any likelihood of instantaneous or rapid load-induced shear failure or any other aspects of service limit failures.

As part of the Federal Highway Administration (FHWA) project, Analysis Procedures for Evaluating Superheavy Load Movement on Flexible Pavements, a comprehensive mechanistic-based analysis approach consisting of several analysis procedures was developed. A summary of the various analysis procedures developed in this study and associated objectives (including related volume number) are summarized in table 1. This report (Volume IX: Appendix H) is the ninth of 10 volumes and presents the procedure for determining the pavement damage–associated cost (PDAC) attributable to SHL movement on flexible pavements.[1–9]

Table 1. Developed analysis procedures to evaluate SHL movements on flexible pavements.

Procedure	Objective
SHL analysis vehicle	Identify segment(s) of the SHL-vehicle configuration that can be regarded as representative of the entire SHL vehicle (Volume III: Appendix B)[3]
Flexible pavement structure	Characterize representative material properties for existing pavement layers (Volume IV: Appendix C and Volume V: Appendix D)[4,5]
SG bearing failure analysis	Investigate instantaneous ultimate shear failure in pavement SG (Volume VI: Appendix E)[6]
Sloped-shoulder failure analysis	Examine the stability of sloped pavement shoulder under an SHL-vehicle movement (Volume VII: Appendix F)[7]
Buried utility risk analysis	Perform risk analysis of existing buried utilities (Volume VIII: Appendix G)[8]
Localized shear failure analysis	Inspect the likelihood of localized failure (yield) in the pavement SG (Volume VI: Appendix E)[6]
Deflection-based service limit analysis	Investigate the development of premature surface distresses (Volume VI: Appendix E)[6]
Cost allocation analysis	Determine PDAC attributable to SHL-vehicle movement (Volume IX: Appendix H)

SG = subgrade.

One of the goals of this project was to present an appropriate mechanistic-based cost allocation methodology for SHL-vehicle movement on flexible pavements. The approach presented in this report allows for the estimation of PDACs due to a single pass of an SHL vehicle. PDAC can be estimated for different SHL-vehicle axle loadings and configurations with due considerations given to locally calibrated pavement-distress models, existing pavement condition, different pavement-repair options, and vehicle miles traveled (VMT).

In this report, a review of highway cost allocation methods as well as the state of the practice in SHL-vehicle permitting in the United States is presented. Next, the adopted cost allocation methodology, which is capable of estimating PDACs due to a single pass of an SHL vehicle, is described in detail. A parametric evaluation that considers several factors that have an influence on the calculation of PDACs is presented next. Finally, a summary of the cost allocation methodology is provided.

CHAPTER 2. REVIEW OF COST ALLOCATION METHODS

A literature review covering different methods of cost allocation was conducted. Although some methods require detailed economic information, others are simpler in regard to data requisites. Each method utilizes measures that relate highway usage to associated costs. Equivalent single-axle loads (ESALs) and VMT are common indicators of total load repetitions imposed by different vehicle classes and are commonly used to relate induced damage per vehicle. A brief discussion about the most common highway cost allocation methods is provided next.

2.1. HIGHWAY COST ALLOCATION METHODS

FHWA and many SHAs regularly conduct highway cost allocation studies to evaluate highway-related expenses attributable to different vehicle classes and to establish highway cost responsibility.[10] The most common methods of cost allocation are incremental, proportional, benefit based, marginal, and costs occasioned. The ultimate goal of these methods is to assign a fair cost-share responsibility to the different highway users.

In the incremental approach, the costs of operating, maintaining, rehabilitating, and constructing highway facilities for the lightest highway users are compared to the costs for larger and heavier traffic classes. Costs that are varied per their association with lighter or heavier traffic are known as incremental costs. Incremental-cost methods are designed to distribute the costs associated with light vehicles among all vehicle classes in proportion to each vehicle's highway usage, whereas only heavier vehicle classes pay for the incremental costs.[10] After 1982, an updated version of the incremental-cost method was conducted in multiple States. That updated version was called the Federal cost allocation method; it is a form of the incremental-cost method with adjustments for some of the expenditures elements in the process.[10,11] The Federal method is based on a consumption principle applied to pavement rehabilitation activities. Contemporaneously with this method, a traditional incremental approach was implemented for some other expenditure elements.

The proportional method distributes highway costs based on vehicle characteristics by using a cost allocation factor such as ESALs and/or VMT. Based on this approach, common construction and maintenance highway costs are distributed proportionally; the higher the VMT or the ESALs, the higher the cost share.

In the benefit-based approach, the benefits are tied to the use of the highway system. Therefore, not only are the direct users of the roadway responsible for the costs, but also all of those who benefit directly from the roadway system. This approach presents several challenges because it is difficult to distinguish nonhighway-user benefits.[11]

In the marginal approach, social costs or added costs related to vehicle trips are associated with highway usage. Air-pollution costs, traffic congestion, noise, marginal pavement costs, and other related expenditures are charged to the highway user.[10] The marginal approach is usually considered when the total or overall highway expenditures are needed. Because of the inclusion of marginal costs to users, it is expected that this method would estimate higher costs to users.[10]

Highway and, most particularly, pavement-damage costs from heavy vehicles have been estimated using cost-occasioned approaches. In this approach, the highway user pays the direct cost his/her vehicle creates; the maintenance, repair, and construction costs can be individually distributed to the respective highway users.[10]

2.2. PAVEMENT-DAMAGE COST MODELS

The National Pavement Cost Model (NAPCOM) is a product of a refined Federal method. In this methodology, increments are categorized as load-related and non-load-related costs. The costs associated with axle loads are obtained through evaluations of different pavement-damage models using mechanistic–empirical (ME) approaches. According to National Cooperative Highway Research Program (NCHRP) synthesis 378, NAPCOM was developed because traditional approaches using simplistic ESALs did not present good correlations with empirical pavement-damage data.[10] The models that NAPCOM is based on considered, among other factors, climatic variations as well as distinct levels of traffic and loads.

NAPCOM has evolved over the years and led to the implementation of simplified models, such as the Pavement Damage Analysis Tool (PaveDAT).[12] This spreadsheet tool uses the same data and relies on the same concepts as NAPCOM to calculate the PDAC for a specific vehicle trip. However, PaveDAT cost models are based on nationally calibrated performance models for typical distresses in flexible pavements that were developed under the NCHRP project. These distress performance models are mostly applicable to flexible pavements built with dense-graded unmodified AC mixtures.[13] Furthermore, traffic-loading input for PaveDAT has to follow FHWA standardized vehicle classification, thus limiting its use with nonstandard vehicles, such as those used during an SHL movement.

The costs of construction and repair attributable to SHL-vehicle movement can be estimated using different methodologies, which often use allocation factors to relate costs to the different vehicle classes. The allocation factor is the joint between costs and usage or damage. For example, Hajek et al. presented a marginal cost allocation procedure to quantify the pavement-associated costs due to proposed changes in trucking regulations in the province of Ontario, Canada.[14] The concept of ESAL was used to account for pavement damage caused by heavier traffic loads. The change in the total number of ESALs per a unit distance per traffic class was used to allocate the costs incurred. Once these parameters were estimated for each traffic class affected by the changes in regulations, the ESALs were converted into costs using the incremental-cost method.

In a Canadian study conducted by Ghaeli et al., the pavement cost allocation was determined through a modified incremental-cost method that used an empirical approach.[15] In this methodology, both the effects of the environment and traffic were considered when modeling pavement condition changes over time. Pavement degradation due to traffic repetitions is represented by number of ESALs per vehicle type, and the environmental effects are calculated as a function of pavement thickness, subgrade (SG) strength, and pavement age. In this method, the road users were classified according to vehicle type, amount of load carried, and road type used.

Table 2 summarizes a number of studies with a focus that was on either the determination of pavement-damage costs or the impact of SHL-vehicle movements on flexible pavements. The cost allocation method and the allocation factor used in these different studies are presented.

Table 2. Summary of cost allocation studies.

Title	Author(s)	Year	Cost Allocation Method	Allocation Factor
Infrastructure Costs Attributable to Commercial Vehicles[16]	Boile, M. et al.	2001	ADOT simplified highway allocation method	ESAL
"Methodology to Determine Load- and Non-Load-Related Shares of Highway Pavement Rehabilitation Expenditures"[17]	Li, Z. et al.	2001	Marginal	ESAL
Estimating the Cost of Overweight Vehicle Travel on Arizona Highways[18]	Strauss, S.H. & Semmens, J.	2006	ADOT simplified highway allocation method	VMT
Pavement Damage From Transit Buses and Motor Coaches[19]	Fekpe, E.	2006	No allocation method utilized	ESAL
"Deterioration Analysis of Flexible Pavements Under Overweight Vehicles"[20]	Sadeghi, J.M. & Fathali, M.	2007	Direct multiplication by allocation factor	Reduction factor of pavement
"A New Approach for Allocating Highway Costs"[21]	Hong, F. et al.	2007	Proportional	ESAL
Correlation Between Truck Weight, Highway Infrastructure Damage and Cost[22]	Timm, D.H. et al.	2007	Benefit cost	ESAL and pavement-life index
Estimating Highway Pavement Damage Costs Attributed to Truck Traffic[23]	Bai, Y. et al.	2010	Synthesized method, including highway economic requirement systems and AASHTO	ESAL
"Process to Estimate Permits Costs for Movement of Heavy Trucks on Flexible Pavements"[24]	Tirado, C. et al.	2010	Cost occasioned	Pavement life–reduction factor
"Index for Estimating Road Vulnerability to Damage From Overweight Vehicles"[25]	Scott, J. & Ferrara, G.P.	2011	No allocation method utilized	Pavement-condition index
"Allocation of Pavement Damage Due to Trucks Using a Marginal Cost Method"[26]	Hajek, J. et al.	1998	Marginal	ESAL-kilometer
Oversize/Overweight Vehicle Permit Fee Study[27]	Prozzi, J. et al.	2012	Proportional	ESAL
"Potential Impacts of Longer and Heavier Vehicles on Texas Pavements"[28]	Weissmann, A.J. et al.	2012	Proportional	ESAL
Rate of Deterioration of Bridges and Pavements as Affected by Trucks[29]	Chowdhury, M. et al.	2013	Proportional	VMT-ESAL
"Evaluation of Superheavy Load Movement on Flexible Pavements"[30]	Chen, X. et al.	2013	Proportional	ESAL

ADOT = Arizona Department of Transportation; AASHTO = American Association of State Highway and Transportation Officials.

Li et al. used the marginal-cost method to determine load- and non-load-related shares of highway pavement rehabilitation expenditures in Indiana.[17] In this study, the concept of present serviceability index–ESAL as the allocation factor was introduced to represent the current condition of the pavement and pavement deterioration due to cumulative use.

Prozzi et al. adopted pavement consumption, which is a modified proportional method, in determining fees that could be charged to overweight (OW) vehicles in Texas.[27] The pavement-consumption methodology is used to determine pavement-damage costs based on additional weight above the legal load limit in Texas.

Chen et al. proposed a cost allocation mechanism based on the predicted pavement damage during an SHL-vehicle movement while considering the estimated costs of repairing the deteriorated pavement.[30] The damage caused by a single pass of the SHL vehicle was compared to that of a reference load by determining an equivalency factor that could be used as a multiplicative factor of repair costs. The vehicle-load equivalency or relative-damage factor was then used to determine cost responsibility.

One limitation of many of the reviewed studies is the use of nationally calibrated pavement-distress prediction models to calculate performance and cost responsibility. For instance, Prozzi et al. revealed that their performance transfer functions were biased due to the use of nationally calibrated performance models.[27] Furthermore, few studies considered the existing pavement condition in the calculation of damage and cost attributed to SHL-vehicle movement. Historically, the calculation of PDAC has assumed that SHL vehicles operate over a new pavement; however, it should be noted that the SHL movement can happen at any time during the life of a pavement, emphasizing the need for a modified cost allocation approach and associated tool that can be used for determining PDAC due to SHL movement and is capable of considering such observed limitations with the existing methods.

2.3. SHL-VEHICLE PERMITTING PRACTICES IN THE UNITED STATES

Papagiannakis recently conducted a review of current SHL-vehicle permitting practices in the United States.[31] According to the study, whereas multiple agencies have adopted a GVW and an axle weight–distance permit scheme, others collect flat fees for single-trip permits. The single-trip permit fee ranged from $25 to $550, regardless of PDAC or any distance indicators.[31] Table 3 summarizes the different SHL permit-fee structures for different SHAs in the United States based on the study conducted by Papagiannakis.[31] This section summarizes the overall findings from this study.

Most SHAs used a weight–distance permit-fee structure by considering tons carried and miles traveled by SHL vehicles. However, there are also SHAs that consider only distance traveled or number of counties traversed (e.g., the Texas Department of Transportation). The research team observed that, in SHAs that employed a weight–distance structure, the fee unit range varied from $0.006 to $0.20 per mi per ton—a wide range that would produce significantly different permit fees from agency to agency.

Table 3. Summary of permit-fee structures in the United States (data from Papagiannakis 2015).[31]

Permit-Structure Type	States	Permit-Fee Examples
Case by case	Alabama, Iowa, Michigan, Nebraska, Rhode Island	At least $20
Weight only	Colorado, Delaware, Georgia, Kentucky, Maine, Maryland, Massachusetts, New Jersey, North Carolina, South Carolina, Vermont	$10 per OW axle $3 per 1,000 lb after 132,000 lb GVW
Weight–distance	Florida, Illinois, Indiana, Louisiana, Minnesota, Mississippi, Missouri, Montana, New Mexico, North Dakota, Ohio, Oklahoma, Oregon, South Dakota, Tennessee, Utah, Virginia, Washington, West Virginia, Wyoming	$0.006 per mi per ton $0.20 per mi per ton $70 plus $3.50 per 5,000 lb per 25 mi $0.05 per mi per 1,000 lb $135 plus $0.04 per ton per mi after 120,000 lb GVW
Distance only	Arizona, Arkansas	$12 per trip < 50 mi > $48 per trip
Fixed fee	Alaska, Idaho, Kansas, Nevada, New Hampshire	$25, $71, $20, $50
Damage related	California, Kansas	Damage fees paid by carrier
Other	New York, Texas	Fee per number of counties traversed

Multiple SHAs charge SHL permit fees on a case-by-case basis. For instance, Alabama charges a nominal permit fee of $100 and applies an additional charge specific to the respective SHL movement. Similarly, Michigan and Nebraska charge extra fees in addition to the $50 and $20 nominal fee, respectively. The extra charges usually depend on the commodities being transported, vehicle dimensions, and axle-configuration characteristics of the SHL vehicle.[31]

There are agencies that implement a weight-only permit-fee structure irrespective of the distance traveled by an SHL vehicle. For example, Colorado collects $10 per OW axle regardless of the distance traveled. North Carolina and South Carolina collect $3 for every 1,000 lb over 132,000 lb GVW with no further consideration given to the distance traveled. New Jersey considers only weight in its permit and charges a base fee of $10 plus $5 for every ton more than 80,000 lb GVW. An additional $5 per ton is charged on single and tandem axles exceeding weights of 22,400 and 34,000 lb, respectively.[31]

Among SHAs that employed a weight–distance structure, it was observed that fee unit ranges and permit-fee structures are significantly variable. For instance, Mississippi charges a flat fee plus $0.05 per mi for each additional 1,000 lb above the legal GVW. Similarly, Ohio charges a flat fee of $135 plus $0.04 per ton and per mi in excess of 120,000 lb. On the other side, the State of Washington charges a flat fee of $25 plus $4.25 for every mile plus $0.50 per every 5,000 lb over 100,000 lb GVW. The variability in permit-fee structures creates different permit fees for SHL vehicles traversing several States.[31]

Arizona and Arkansas consider only distance in their permit-fee structures. Arizona charges $12 for single-trip permits for vehicles traveling less than 50 mi and $48 for vehicles traveling more than 50 mi. Similarly, Arkansas charges a nominal fee of $17 and extra charges ranging from $8 to $16 depending on the distance traveled.[31]

Among States that charge a single flat fee without consideration of distance traveled, axle weight, or GVW are Nevada, Idaho, Kansas, and California. Nevada charges $25 per single trip. Idaho and Kansas charge $71 and $50, respectively, with no specific or additional fees. California implements a flat permit fee of $16, but the carrier pays a fee for any infrastructure repairs.[31]

Two States use a permit-fee structure that cannot be grouped in any of the aforementioned categories. New York charges a permit fee ranging from $40 to $360 depending on the commodity being transported plus an analysis fee depending on the GVW. On the other hand, Texas charges a flat fee of $90 plus a fee depending on the number of counties being traversed plus maintenance and supervision fees for SHL vehicles.[31]

Most States do not provide a particular regulation or structure for the issuance of annual-trip or multitrip permits. For instance, Nevada charges $60 per annual-trip permit. Whereas Kentucky charges $500 per annual-trip permit, Missouri and Wisconsin charge fees ranging from $300 to $850.

As part of the application process, multiple agencies request or conduct empirical or ME pavement analyses when SHL vehicles are involved. However, the main objective of such analyses is to evaluate the structural capacity of the pavement section. Consequently, the analyses are not focused on determining a permit fee that is directly associated with the pavement damage produced by a single pass of an SHL vehicle. Therefore, a reliable approach for estimating PDAC due to SHL vehicles that can consider the various influential factors is needed.

CHAPTER 3. PDACs

The goal of this chapter is to present a mechanistic-based cost allocation approach that will determine PDACs due to a single pass of an SHL vehicle. Figure 1 shows the flowchart of the overall approach developed as part of this FHWA project, Analysis Procedures for Evaluating Superheavy Load Movement on Flexible Pavements. In general, the approach consists of four major components: ultimate failure analyses, buried utility risk analysis, service limit analyses, and cost allocation analysis. It should be noted that mitigation strategies may be needed at any stage of the evaluation process when the calculated results fail to meet the imposed requirements.

The approach begins with a risk analysis of instantaneous or rapid load-induced ultimate shear failure. The SG bearing failure analysis investigates the likelihood of general bearing capacity failure under the SHL vehicle within the influenced zone of the SG layer. The sloped-shoulder failure analysis examines the bearing capacity failure and the edge slope stability associated with the sloping ground under the SHL-vehicle movement. Once the ultimate failure analyses are investigated and ruled out, whenever applicable, a buried utility risk analysis is then conducted. In this analysis, the induced stresses and deflections by the SHL vehicle on buried utilities are evaluated and compared to established design criteria. Then, if no mitigation strategies are needed, service limit analyses for localized shear failure and deflection-based service limit are conducted. The localized shear failure analysis investigates the possibility of failure at the critical location on top of the SG layer under the SHL vehicle. The deflection-based service limit analysis assesses the magnitude of the load-induced pavement deflections during the SHL movement. For instance, this analysis may suggest the need for mitigation strategies in order to meet the imposed acceptable surface deflection limits.

After successfully completing ultimate failure analyses, buried utility risk analysis, and service limit analyses, a cost allocation analysis is conducted. This analysis involves the assessment of the incremental pavement damage and PDACs resulting from the SHL movement on a flexible pavement. Section 3.1 summarizes the overall cost allocation methodology for SHL movements on flexible pavements along with the various steps involved in this analysis. A summary of the inputs needed to undertake such an analysis is also presented. Then, a step-by-step example following the proposed cost allocation methodology is illustrated for a permitted SHL vehicle.

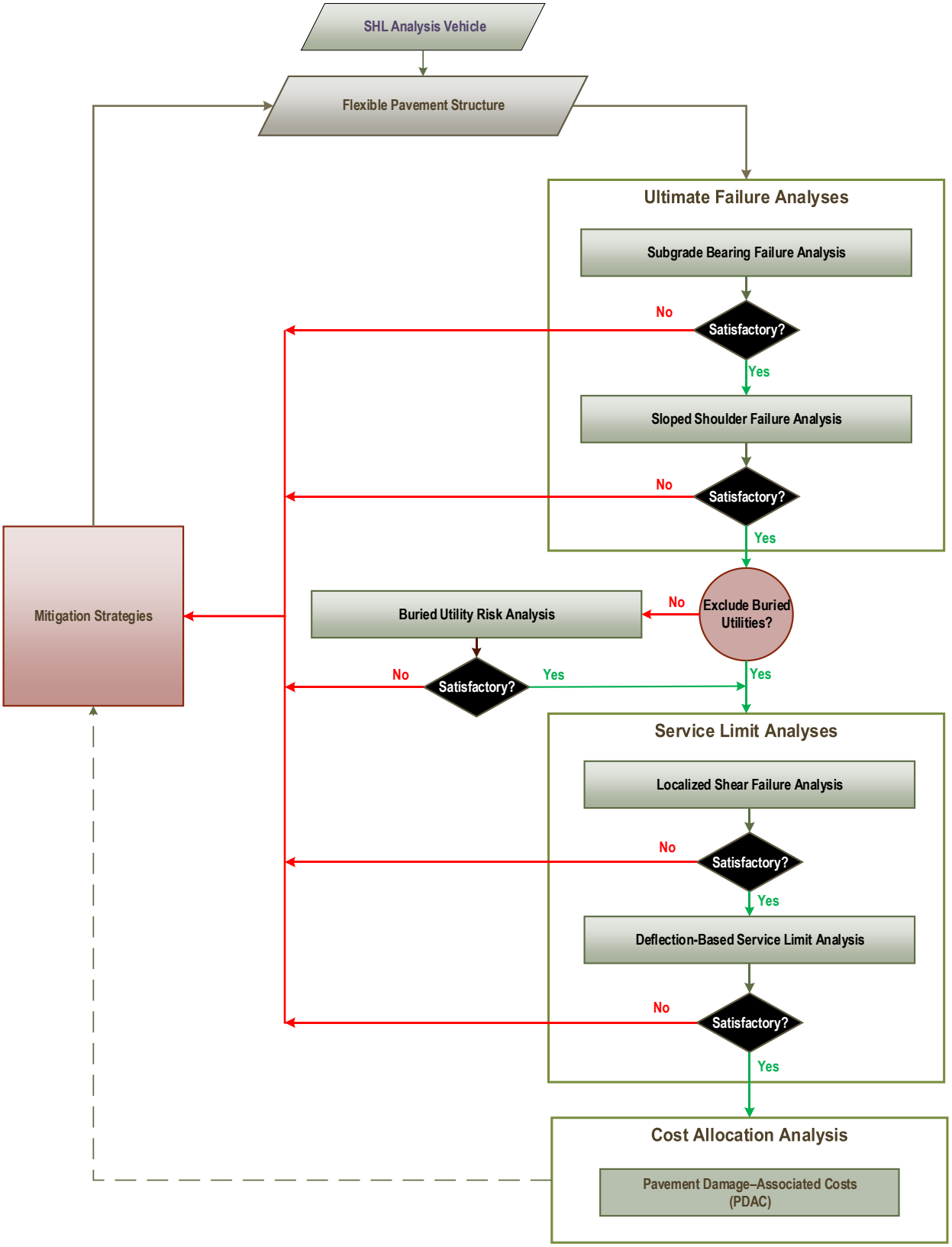

Figure 1. Flowchart. Overall SHL-vehicle analysis methodology.

3.1. COST ALLOCATION METHODOLOGY FOR SHL MOVEMENT

The approach suggested by Tirado et al., who implemented the highway cost-occasioned method to estimate PDACs using ME analysis, was adopted in this project.[24] This cost allocation approach estimates pavement-damage costs based on vehicle axle loading and configuration and considers the predicted pavement life reduction (LR) due to a single pass of the evaluated SHL vehicle. With this method, different pavement distress models, pavement-repair options, and any axle configuration can be implemented. The present worth value (PWV) of repairing costs and VMT are also needed inputs of the process.[24] The approach presented by Tirado et al. was revised in this study to consider the current condition of the pavement at the time of the pass.[24] Consequently, lower PDACs will be estimated for an SHL pass occurring on a pavement section with lower remaining life (i.e., a pavement section that has already been subjected to a percentage of its original design traffic).

3.2. PAVEMENT PERFORMANCE–PREDICTION MODELS

Pavement-damage predictions are an essential element of the proposed PDAC approach in section 3.1. Any realistic damage predictions need to rely on proper locally calibrated distress-performance models to appropriately estimate pavement damage under both SHL and reference vehicles.[32] The reference vehicle is designated by the respective SHA. The pavement damage caused by the reference vehicle is used in the PDAC analysis as a baseline and for comparison. A typical 18-wheel truck with a GVW of 80,000 lb with one steering axle weighing 12,000 lb and two tandem axles each weighing 34,000 lb is usually used as the reference vehicle. Critical pavement responses, as required by the corresponding performance models, need to be determined for each of the axle groups associated with the evaluated SHL and reference vehicles.

The locally calibrated performance models are employed to estimate pavement damage associated with each axle group. The number of axle-group repetitions to specific rehabilitation failure criteria are estimated using the appropriate equations. For instance, the model equations for AC rutting and AC bottom–up fatigue cracking shown in figure 2 and figure 3, respectively, are implemented as part of this project. These equations are implemented in the American Association of State Highway and Transportation Official's (AASHTO's) *Mechanistic–Empirical Pavement Design Guide* (MEPDG) and the associated AASHTOWare® Pavement ME software.[13,33]

$$\frac{\varepsilon_p}{\varepsilon_r} = 10^{\beta_{r1}k_{r1}} T^{\beta_{r2}k_{r2}} {N_r}^{\beta_{r3}k_{r3}}$$

Figure 2. Equation. AC-rutting performance model.

Where:

ε_p = plastic strain at the middepth of the AC layer.
ε_r = resilient strain at the middepth of the AC layer.
T = temperature at the middepth of the AC layer.
N_r = number of load applications to AC permanent deformation failure.
k_{r1} = AC permanent deformation calibration factor.
k_{r2} = AC permanent deformation exponent calibration factor for T.
k_{r3} = AC permanent deformation exponent calibration factor for N_r.

β_{r1} = AC permanent deformation local calibration factor.
β_{r2} = AC permanent deformation exponent local calibration factor for T.
β_{r3} = AC permanent deformation exponent local calibration factor for N_r.

$$N_f = \beta_{f1} k_{f1} \left(\frac{1}{\varepsilon_t}\right)^{\beta_{f2} k_{f2}} \left(\frac{1}{E_{AC}}\right)^{\beta_{f3} k_{f3}}$$

Figure 3. Equation. AC fatigue-cracking performance model.

Where:
N_f = number of load applications to fatigue cracking failure.
ε_t = maximum tensile strain at bottom of the AC layer.
E_{AC} = AC-layer dynamic modulus.
k_{f1} = fatigue cracking calibration factor.
k_{f2} = fatigue cracking exponent calibration factor for ε_t.
k_{f3} = fatigue cracking exponent calibration factor for E_{AC}.
β_{f1} = fatigue cracking laboratory calibration factor.
β_{f2} = fatigue cracking laboratory exponent calibration factor for ε_t.
β_{f3} = fatigue cracking laboratory exponent calibration factor for E_{AC}.

The MEPDG performance model to estimate rutting within unbound materials (e.g., crushed aggregate base (CAB) and SG) is also implemented as part of this study.[13] The performance model equations are presented in figure 4 through figure 7.

$$\delta(N) = \beta_{s1}\, k_{s1} \left(\frac{\varepsilon_0}{\varepsilon_r}\right) e^{-\left(\frac{\rho}{N}\right)^{\beta}} \varepsilon_v h_s$$

Figure 4. Equation. Rutting in unbound materials performance model.

Where:
$\delta(N)$ = permanent deformation corresponding to N-load for unbound materials.
N = number of axle group repetitions.
k_{s1} = unbound materials calibration factor.
β_{s1} = unbound materials local calibration factor.
ε_o = intercept determined from laboratory repeated load permanent deformation tests.
β = power parameter for material property.
ρ = material property parameter.
ε_v = calculated vertical resilient strain in the unbound-material layer.
h_s = the thickness of the unbound-material layer.

$$\log \beta = -0.61119 - 0.017638\, W_c$$

Figure 5. Equation. Determination of β factor for unbound materials.

Where W_c is water content.

$$\log \rho = 0.622685 + 0.541524\, W_c$$

Figure 6. Equation. Determination of ρ factor for unbound materials.

$$W_c = 51.712\left[\left(\frac{M_r}{2{,}555}\right)^{\frac{1}{0.64}}\right]^{-0.3586\ GWT^{0.1192}}$$

Figure 7. Equation. Determination of water content in unbound materials.

Where:

GWT = depth of ground water table.
M_R = resilient modulus of the unbound layer.[13]

The allowable number of repetitions for a given vehicle was estimated using Miner's rule as shown in figure 8.[34]

$$\frac{1}{N_{failure}} = \frac{1}{N_{1:failure}} + \frac{1}{N_{2:failure}} + \frac{1}{N_{3:failure}} + \cdots + \frac{1}{N_{i:failure}}$$

Figure 8. Equation. Miner's rule to determine allowable number of repetitions for the entire vehicle.

Where:

$N_{failure}$ = estimated number of passes of SHL or reference vehicles to the threshold failure.
$N_{i:failure}$ = estimated number of passes to the same threshold failure for the individual axle groups within the SHL or reference vehicle.

In mechanistic analysis of flexible pavements, each set of axle combinations (i.e., single, tandem, or tridem axles) is treated as one axle group. Subsequently, for each axle group, the maximum pavement response is determined and used for pavement-performance prediction. In fact, the performance models are calibrated based on the estimated maximum response (i.e., single response value) for each axle group. In such an undertaking, only a single maximum pavement response for the axle group is required for pavement distress predictions.[13]

The same principle is applicable to SHL vehicles, which typically have nonstandard axle and tire configurations. Thus, the closely spaced axles (spacing less than or equal to 60 inches) with identical properties (i.e., similar axle loading, axle spacing, and tire configuration) are combined into a number of single-axle groups. Therefore, only the peak response (e.g., maximum tensile strain at the bottom of the AC layer) for each axle group is used with the associated pavement-performance model for distress prediction.

Previous studies revealed that, when the spacing between two adjacent axles is more than 60 inches, the pavement responses under one of the axles have limited interaction by the adjacent axle load (i.e., minimal interaction among the two adjacent axles).[35] Such criteria for axle spacing can be employed to define the various axle groups for an SHL vehicle. Accordingly, two or more axles with identical properties and axle spacing less than 60 inches can be classified as though they belong to a single group of axles. For instance, figure 9 shows a schematic of the axle configuration for a given SHL vehicle. Using the 60-inch criteria for axle spacing, the SHL can be divided into seven axle groups—a steering single axle (A group), a tridem axle (B group), and five tandem axles (C, D, E, F, and G groups). As an example, figure 10 through figure 12 show the tensile strain history response at the bottom of the AC layer determined using the

3D-Move Analysis software for the defined axle groups.[36] The SHL vehicle was assumed to travel over a flexible pavement structure that consisted of 6 inches of AC over 10 inches of CAB over SG (table 4). Table 5 summarizes the critical (maximum) tensile strains at the bottom of the AC layer under the various SHL axle groups. A vehicle travel speed of 45 mph and an analysis temperature of 70 °F for the AC layer were used in this evaluation.

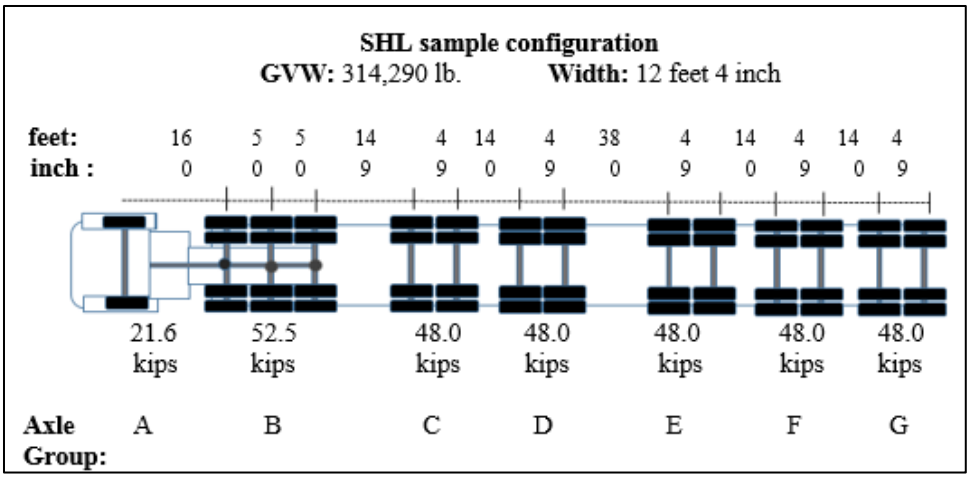

Figure 9. Illustration. Example of an SHL-vehicle configuration.

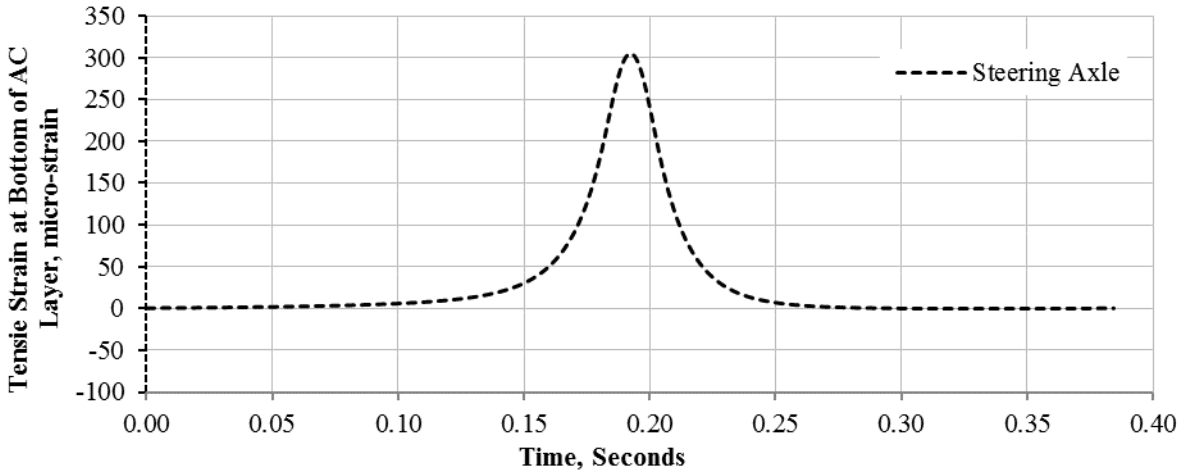

Figure 10. Graph. Tensile strain response history at the bottom of AC layer for axle group A (single axle).

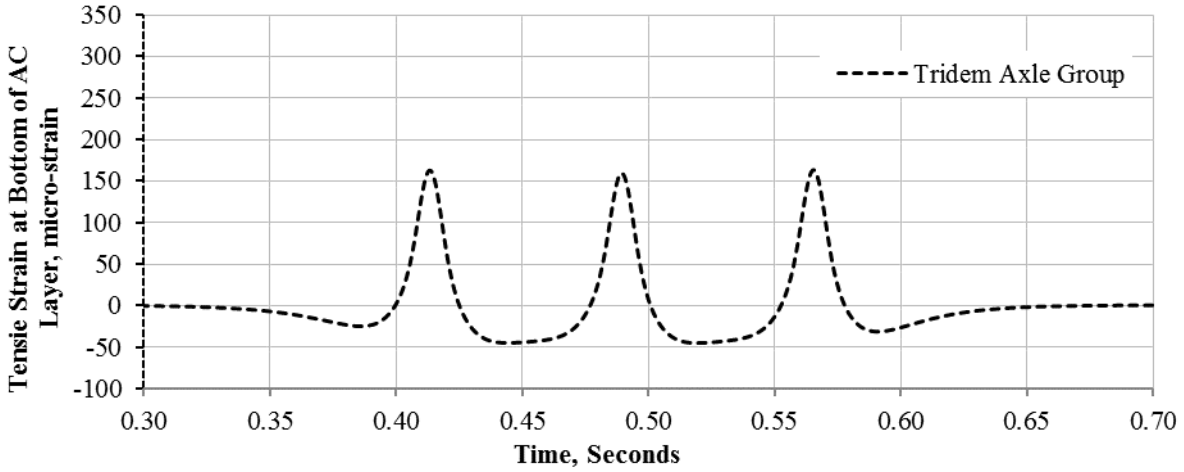

Figure 11. Graph. Tensile strain response history at the bottom of AC layer for axle group B (tridem axle).

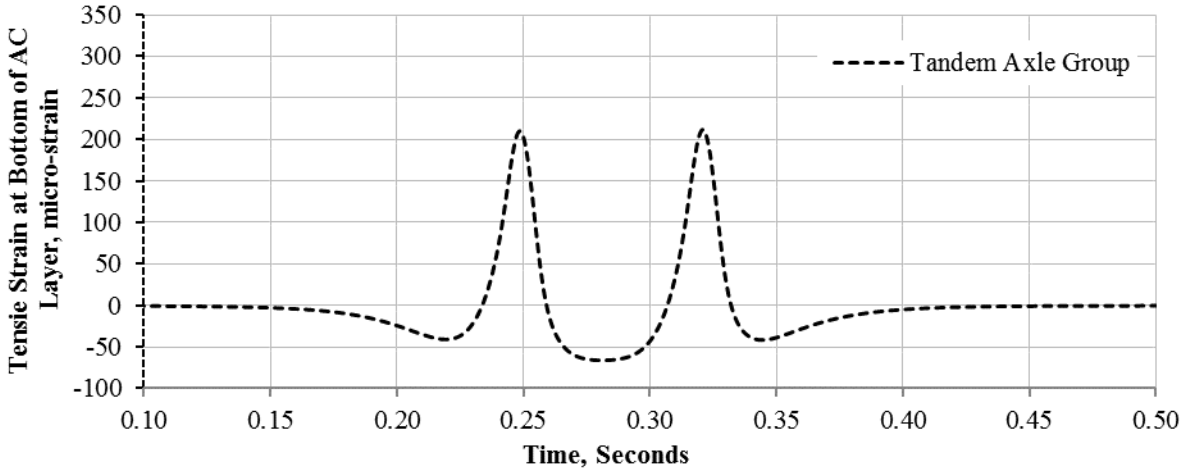

Figure 12. Graph. Tensile strain response history at the bottom of AC layer for axle groups C, D, E, F, and G (tandem axles).

Table 4. Pavement structure used in the cost allocation analysis example.

Pavement Layer	Thickness (Inches)	Property	Modulus (psi)	Poisson's Ratio
AC	6	Viscoelastic	E_{AC}	0.35
CAB	10	Linear elastic	30,000	0.40
SG	Infinite	Linear elastic	15,000	0.40

Table 5. Critical (maximum) ε_t by axle group.

Axle Group	Axle Type	Axle Spacing	Number of Wheels	Axle Weight (lb)	Maximum ε_t (Microstrain)
A	Steering	Not applicable	2	21,600	290.6
B	Tridem	5 ft 0 inches	12	52,500	163.5
C	Tandem 1	4 ft 9 inches	8	48,038	211.2
D	Tandem 2	4 ft 9 inches	8	48,038	211.2
E	Tandem 3	4 ft 9 inches	8	48,038	211.2
F	Tandem 4	4 ft 9 inches	8	48,038	211.2
G	Tandem 5	4 ft 9 inches	8	48,038	211.2

In the case of a tridem axle group (figure 11), there are three distinct peaks in tensile strain response (one peak strain under each of the three axles within the tridem axle). Although the peak values for the tensile strain are similar, the tridem axle is counted as one pass, and the allowable number of load repetitions to fatigue failure is calculated using the maximum strain value induced by the entire tridem axle group. Note that the same assumption is used during the calibration process of the performance models and distress transfer functions in the MEPDG.[13] If all the peak strains in a response history are individually considered for distress prediction, the analysis would severely underestimate the pavement performance under the SHL vehicle, resulting in improper (higher) estimates for pavement damage and associated costs.

There are cases in which an SHL-vehicle configuration has several trailers, or dollies, comprising multiple tires and complex, specialized axle arrangements. This type of configuration requires the determination of the nucleus, a representative group of tires that presents the highest vertical stress distribution at a selected depth of interest. In this case, the SHL vehicle is divided into one or more nuclei that, when repeated, will cover the entire SHL-vehicle configuration. The number of nucleus repetitions within the SHL-truck domain is considered for pavement damage–cost calculation instead of individual axle repetitions. It should be noted that, when the spacing between two trailers is greater than 60 inches, they are treated as independent groups by defining a separate nucleus for each group.

Figure 13 presents a sample of an SHL configuration in which a series of trailers are combined. This configuration comprises 224 tires. After determining the nucleus, it was found that a group of 16 nearby tires (4 by 4 tires) produces the highest stress levels under this SHL configuration. In this case, this group of tires is referred to as the nucleus. The entire SHL configuration is then divided into 14 identical nuclei. Therefore, the single maximum response under the 16 tires within the nucleus domain is used in the pavement-performance and cost-methodology calculations, assuming that the total number of repetitions is 14.

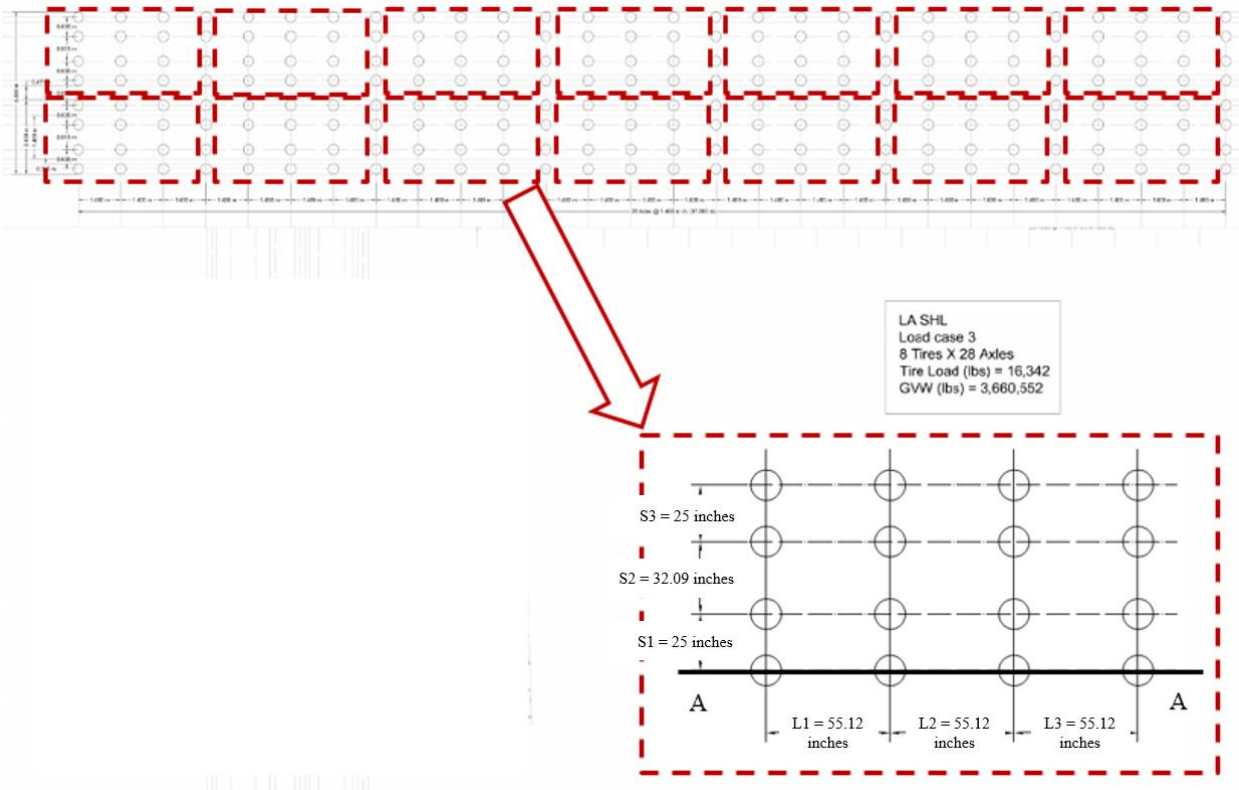

Figure 13. Sketch. Nonstandard SHL-vehicle and -nucleus configuration.

3.3. METHODOLOGY STEPS

To estimate a PDAC, distress performance models are needed to predict pavement performance and estimate pavement damage under both SHL and reference vehicles. The estimated damage is then used to calculate PDACs due to a single pass of the SHL vehicle. The overall flowchart for the cost allocation–analysis method is presented in figure 14, and it can be summarized in the following 11 steps.[24]

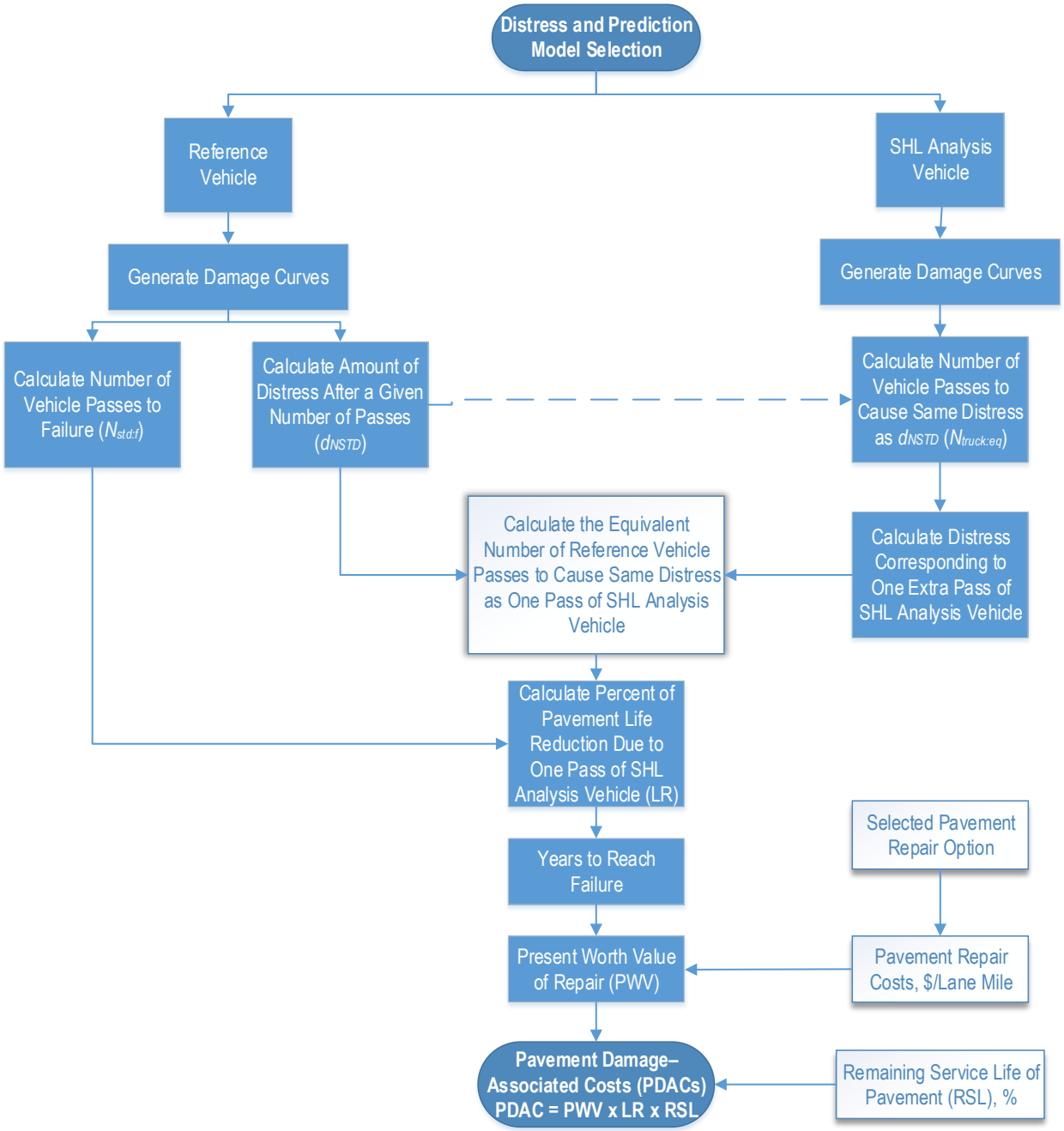

Modified from © 2010 Tirado et al. Reprinted by permission from SAGE Publications, Inc.

Figure 14. Flowchart. Overall approach for the estimation of pavement damage and allocated cost.[24]

1. Damage curves based on a specific performance prediction model with a specific threshold are first developed for SHL and reference vehicles to relate predicted distress to vehicle passes.

2. The predicted number of reference-vehicle passes to reach the established failure threshold ($N_{std:f}$) is determined.

3. The amount of distress after a specific number of passes (d_{Nstd}) (e.g., 10,000 passes ($d_{Nstd:10,000}$)) of the reference vehicle is estimated from the reference-vehicle damage curve.

4. The number of SHL-vehicle passes to cause the same amount of distress as $d_{Nstd:10,000}$ ($N_{truck:eq}$) is determined from the SHL-vehicle damage curve.

5. The damage caused by an extra pass of the SHL vehicle after $N_{truck:eq+1}$ ($d_{truck:eq+1}$) is determined from the SHL-vehicle damage curve.

6. The number of additional passes of the equivalent reference vehicle to cause $d_{truck:eq+1}$ ($\Delta N_{std:eq}$) is estimated from the reference-vehicle damage curve.

7. The percentage of pavement LR is obtained from one pass of the SHL vehicle and calculated as shown in figure 15.

$$LR = \frac{\Delta N_{std:eq}}{N_{std:f}}$$

Figure 15. Equation. Percentage of pavement LR.[24]

8. The pavement service life (n) in years is determined as a function of the actual average annual daily truck traffic (AADTT) and $N_{std:f}$ as shown in figure 16.

$$n = \frac{N_{std:f}}{AADTT \times 365}$$

Figure 16. Equation. Calculation of *n*. [24]

9. The *PWV* of repairing the pavement when the failure threshold is reached is calculated as shown in figure 17.

$$PWV = \frac{Cost}{(1 + Discount\ Rate)^n}$$

Figure 17. Equation. *PWV* of repairing the pavement when reaching failure threshold.[24]

Where:

Cost = pavement-repair cost in dollars per lane-mile.
Discount Rate = real discount rate that reflects the time value of money with no inflation premium (should be used in conjunction with noninflated-dollar cost estimates of future investments).

10. To consider the remaining service life (RSL) of the pavement at the time of the SHL movement, the *RSL* factor is introduced and calculated following the equation shown in figure 18. Here, the *Year of SHL Pass* is defined as the year when the SHL movement is expected to take place. The *Year of Last Repair* is the year when the last structural pavement repair took place. Finally, the *Year of Next Repair* is defined as the year of the next scheduled structural pavement repair.

$$RSL = 1 - \frac{Year\ of\ SHL\ \ Pass - Year\ of\ Last\ Repair}{Year\ of\ Next\ Repair - \ Year\ of\ Last\ Repair}$$

Figure 18. Equation. Calculation of *RSL* factor.

11. *PDAC* is calculated based on the product of *PWV*, *LR*, and *RSL* as shown in figure 19.

$$PDAC = PWV \times LR \times RSL$$

Figure 19. Equation. Calculation of *PDAC*.

3.4. INPUTS NEEDED FOR COST ALLOCATION ANALYSIS

As presented in previous sections, multiple variables are needed to determine PDAC using the proposed methodology. These values can be classified as general inputs and inputs specifically related to the existing pavement layers. Pavement-damage predictions are key elements of the proposed mechanistic-based methodology. Thus, critical pavement responses at different locations within the pavement structure are determined for each of the axle groups identified for the SHL and reference vehicles. Locally calibrated performance models are used to estimate pavement damage associated with each axle group. Table 6 through table 8 present a complete summary of all necessary inputs for conducting the cost allocation analysis.

Table 6. List of inputs for cost allocation analysis: general.

General Input Description	Unit
Repair-activity costs	Dollars/lane-mile
Discount rate	Percent
Number of repetitions of reference vehicle prior to the pass of SHL vehicle	—
AADTT	—
SHL-vehicle operating speed	Miles per hour

—No unit.

Table 7. List of inputs for cost allocation analysis: AC layer.

AC-Layer Input Description	Unit
Maximum vertical strains at the middle of AC layer under reference-vehicle axle groups and SHL-vehicle nuclei (or axle groups)	Inch/inch
Permanent deformation calibration constants	—
Allowable permanent deformation in AC layer	Inch
Maximum tensile strains at bottom of AC layer under reference-vehicle axle groups and SHL-vehicle nuclei (or axle groups)	Inch/inch
Allowable fatigue cracking in AC layer	$Feet^2$
Bottom–up fatigue cracking performance model calibration constants	—
T	Degrees Fahrenheit

—No unit.

Table 8. List of inputs for cost allocation analysis: unbound layer.

Unbound-Layer Input Description	Unit
Maximum vertical strains at the middle of unbound layers under reference-vehicle axle groups and SHL-vehicle nuclei (or axle groups)	Inch/inch
Allowable permanent deformation in each of the unbound layers	Inch
Unbound materials permanent deformation performance model calibration constants	—

—No unit.

3.5. ILLUSTRATION EXAMPLE FOR PDAC CALCULATION

To illustrate the proposed cost allocation methodology, the step-by-step calculations are presented for PDACs of an SHL vehicle with a GVW of 500,825 lb. The SHL movement with a VMT of 22 mi was proposed to happen in southern Nevada. Figure 20 illustrates the SHL vehicle's characteristics, including axle load and configuration, vehicle width, and VMT. The cost allocation methodology requires the prediction of pavement damage under both the SHL and the designated reference vehicles using their respective critical responses. In this section, the methodology is demonstrated for the case of AC permanent deformation. It should be noted that the width of the SHL vehicle, which will span over two lanes, is 20 ft 5 inches. Similarly, information about the reference vehicle used in the calculation of PDACs is also shown in figure 21. The reference vehicle was a 5-axle truck with 18 wheels and a GVW of 80,000 lb.

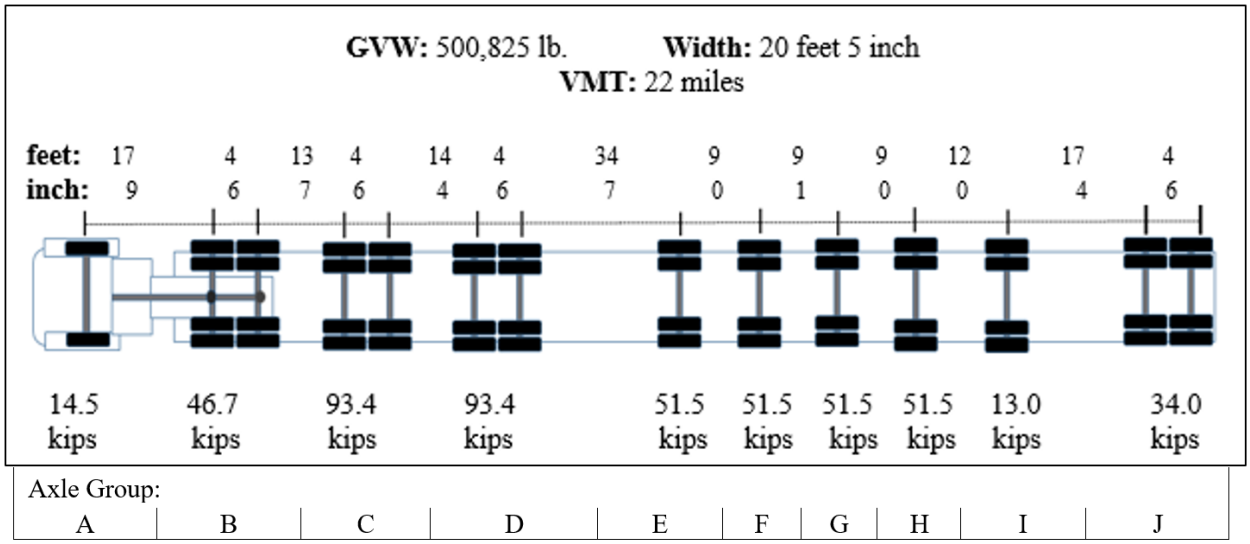

Figure 20. Illustration. SHL-vehicle configuration.

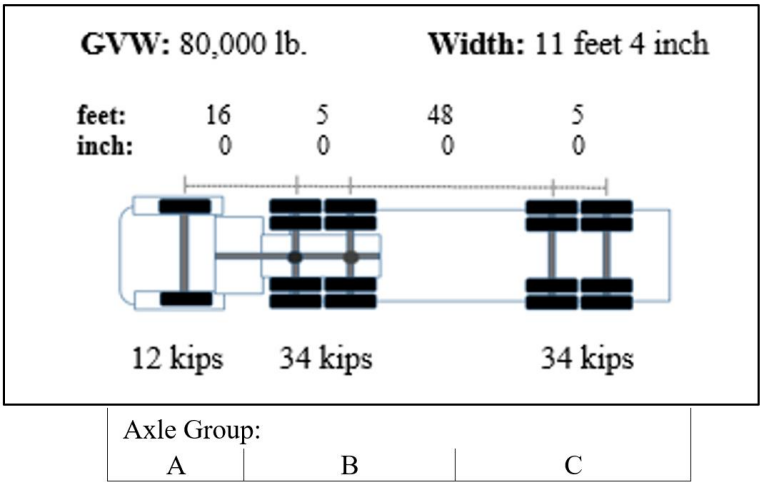

Figure 21. Illustration. Reference-vehicle configuration.

The critical pavement responses under the SHL and reference vehicles were determined using the 3D-Move Analysis software.[36] In this example, it is assumed that the SHL vehicle will travel over a flexible pavement structure consisting of 6 inches of AC over 10 inches of CAB over SG as presented in table. The AC layer consisted of a polymer-modified dense-graded asphalt mixture using PG76-22P asphalt binder. This asphalt mixture is typically used by the Nevada Department of Transportation in southern Nevada. The measured E_{AC} of the asphalt mixture was used in this analysis.

Table 9 summarizes the maximum vertical strains in the middle of the AC layer under both the SHL and reference vehicles. These responses are needed for the estimation of permanent deformation in the AC layer. An operational vehicle speed of 35 mph and an AC analysis temperature of 110 °F were used in this example. The high temperature used is considered a representative temperature for the AC layer during a day in June. Following the steps presented in section 3.1.2, PDACs for the SHL vehicle presented in figure 20 were determined. It should be noted that permanent deformation calibration constants for southern Nevada were implemented in this example for pavement-damage estimation.

Table 9. Critical responses under SHL and reference vehicles traveling at 35 mph.

Axle	Axle Group	Axle Spacing (Inches)	Number of Wheels	Axle Weight (lb)	Maximum Vertical Strain in the Middle of AC at 110 °F (Microstrain)
SHL-vehicle steering	A	—	2	14,500	354.8
SHL-vehicle tandem	B	54	8	46,725	354.8
SHL-vehicle tandem	C	54	8	93,400	394.7
SHL-vehicle tandem	D	54	8	93,400	394.7
SHL-vehicle single dual	E	—	4	51,450	384.2
SHL-vehicle single dual	F	—	4	51,450	384.2
SHL-vehicle single dual	G	—	4	51,450	384.2
SHL-vehicle single dual	H	—	4	51,450	384.2
SHL-vehicle single dual	I	—	4	13,000	302.6
SHL-vehicle tandem	J	54	8	34,000	333.9
Reference-vehicle steering	A	—	2	12,000	373.6
Reference-vehicle tandem	B	60	8	34,000	333.9
Reference-vehicle tandem	C	60	8	34,000	333.9

—Not applicable.

The PDAC based on AC permanent deformation for the studied SHL-vehicle movement is calculated following the 11 steps described in section 3.3.

1. The locally calibrated constants for unbound materials in southern Nevada are used in this analysis. Figure 22 presents the damage curves related to AC permanent deformation for both SHL and reference vehicles. For a fixed permanent deformation, a significantly lower number of passes is expected for the SHL vehicle compared to the reference vehicle.

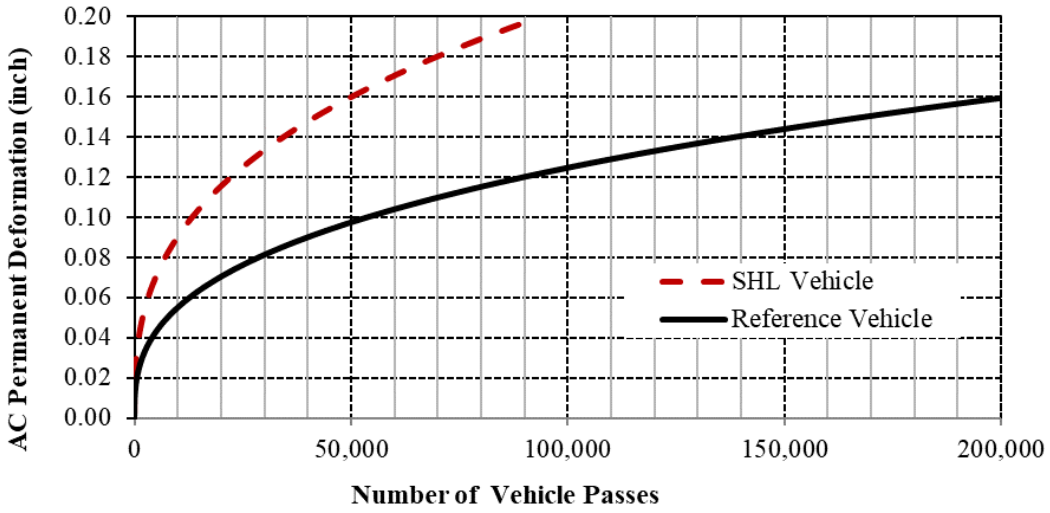

Figure 22. Graph. AC permanent deformation damage curves under SHL and reference vehicles.

2. $N_{std:f}$ for a failure criterion of 0.15 inch is calculated to be 170,000 passes (figure 23).

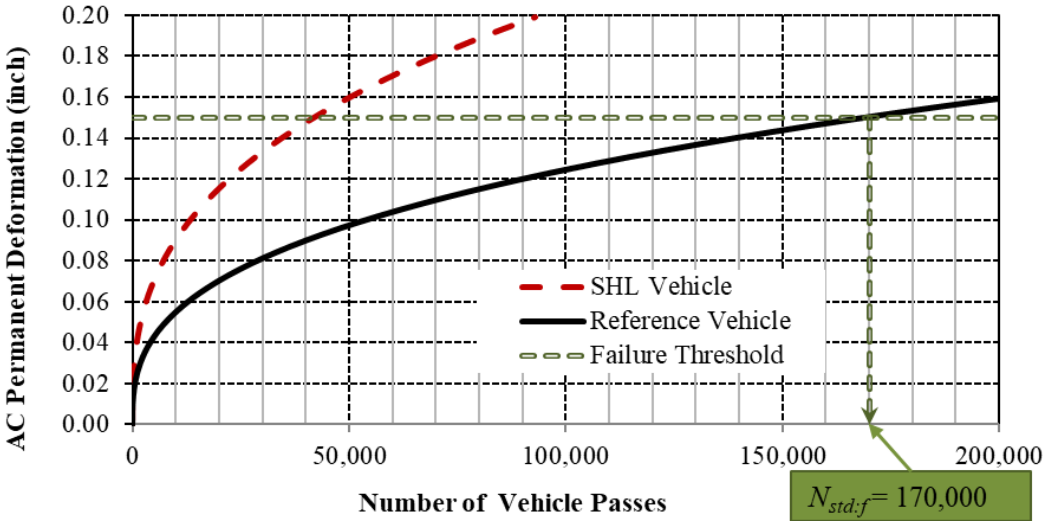

Figure 23. Graph. Number of reference-vehicle passes to failure.

3. $d_{Nstd:10,000}$ is determined to be 0.054 inch as shown in figure 24.

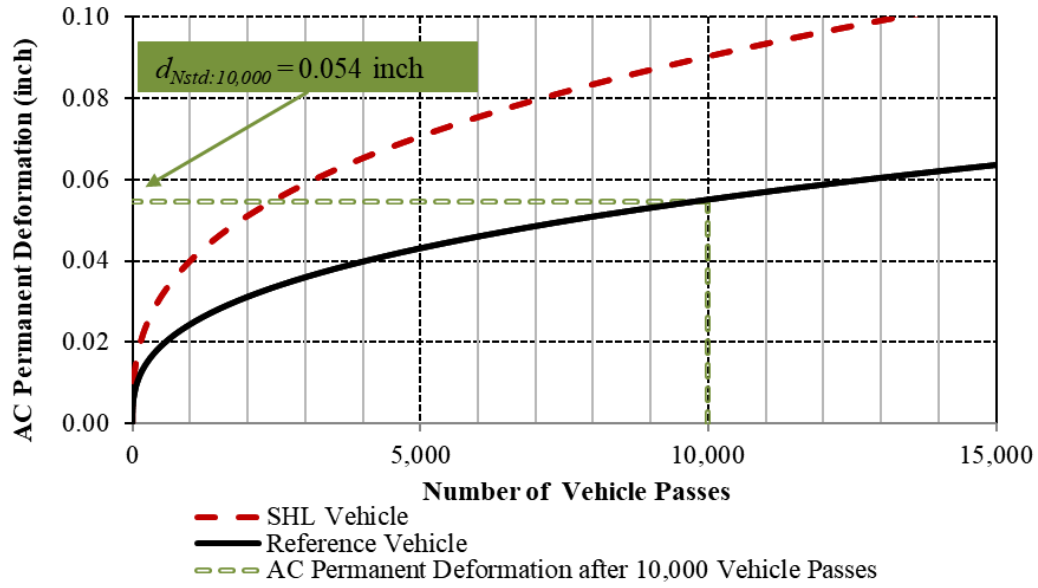

Figure 24. Graph. AC permanent deformation after 10,000 passes of reference vehicle.

4. $N_{truck:eq}$ (0.054 inch) is determined to be 2,350 passes as shown in figure 25.

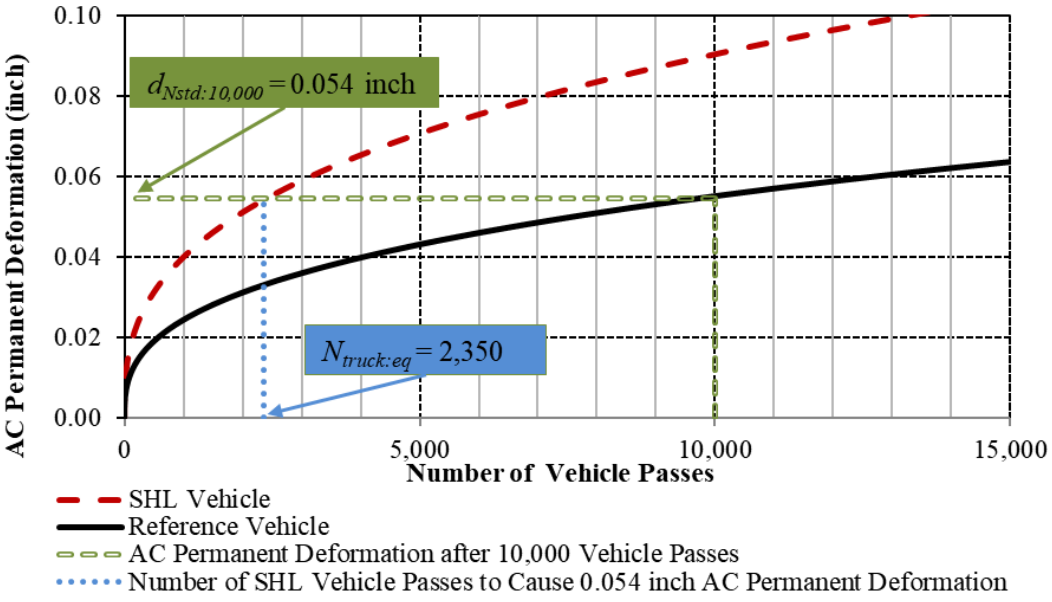

Figure 25. Graph. $N_{truck:eq}$.

5. $d_{truck:eq+1}$ after 2,350 passes is determined, based on the SHL-vehicle damage curve, to be 0.056 inch as shown in figure 26.

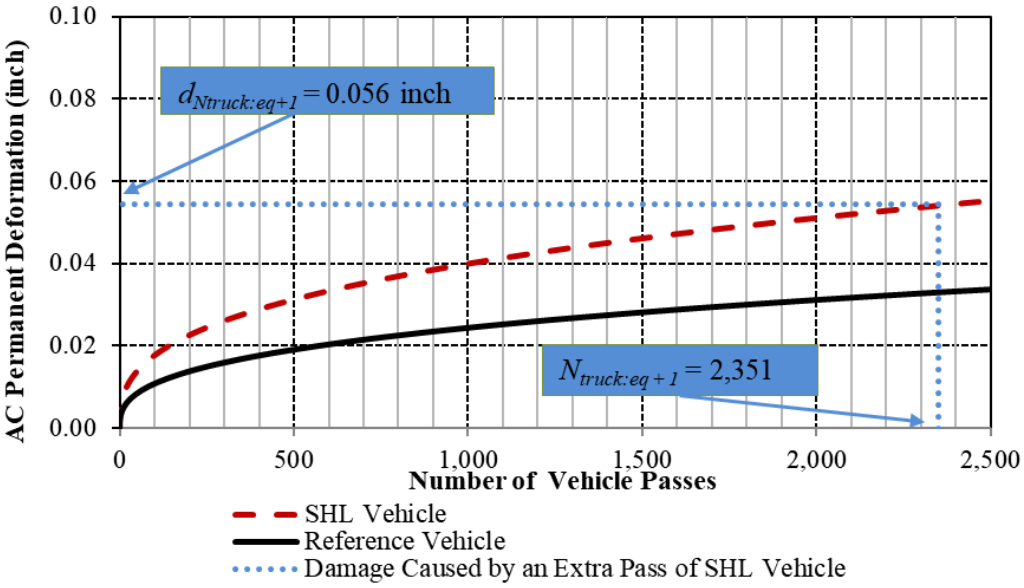

Figure 26. Graph. AC permanent deformation after $d_{truck:eq+1}$ (2,351).

6. The number of additional passes of the reference vehicle to cause $d_{truck:eq+1}$ (i.e., 0.056 inch) after 10,000 passes of the reference vehicle is determined to be 2.89 as shown in figure 27.

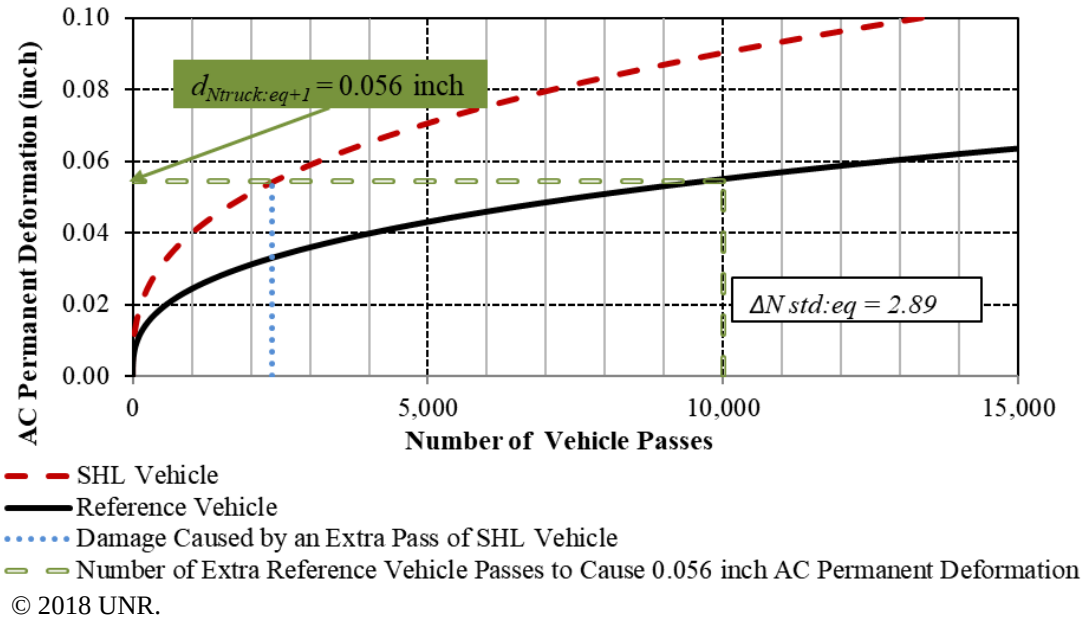

Figure 27. Graph. Additional number of reference-vehicle passes to reach $d_{truck:eq+1}$ (0.056 inch).

7. The pavement *LR* is then calculated to be 0.000017 as shown in figure 28.

$$LR = \frac{2.89}{170{,}000} = 0.000017$$

Figure 28. Equation. Calculation of pavement *LR*.

8. The pavement service life in years is determined assuming an AADTT of 100.

$$n = \frac{170{,}000}{100 \times 365} = 4.65$$

Figure 29. Equation. Calculation of pavement service life in years.

9. The *PWV* was obtained assuming a pavement-repair cost per lane-mile of $350,000 and a discount rate of 2.0 percent.

$$PWV = \frac{350{,}000}{(1 + 0.02)^{4.65}} = 319{,}212$$

Figure 30. Equation. Calculation of *PWV*.

10. An *RSL* of the pavement section is assumed to be 90 percent.

11. Calculation of the *PDAC* is shown in figure 31 and figure 32 in dollars per lane-mile and dollars per trip, respectively.

$$PDAC = (319{,}212)(0.000017)(0.9) = 4.88$$

Figure 31. Equation. Calculation of PDAC in dollars per lane-mile.

$$PDAC = (4.88)(2)(22) = 214.72$$

Figure 32. Equation. Calculation of *PDAC* in dollars per trip for an SHL vehicle spanning two lanes and a VMT of 22 mi.

Figure 32 shows that the total PDAC based on AC permanent deformation for the studied SHL-vehicle movement was approximately $215. It is important to note that the calculated PDAC corresponds to the SHL vehicle traveling at a speed of 35 mph and at an estimated temperature in the AC layer of 110 °F during the movement.

In summary, although several factors might influence the analysis, the presented example highlights the proposed procedure to calculate PDACs due to a single pass of the evaluated SHL vehicle on a flexible pavement. In particular, the selection of the pavement distresses of interest along with their associated locally calibrated performance models becomes another critical factor in the appropriate determination of PDACs by SHAs.

CHAPTER 4. PARAMETRIC EVALUATION

In this section, the influence of selected factors on the calculated PDAC is evaluated. The SHL vehicle presented in figure 20 and the pavement structure shown in table 4 are considered the control SHL vehicle and control section, respectively. In this evaluation, all input values as presented in section 3.2 were kept constant unless otherwise noted. The AC permanent deformation and the AC bottom–up fatigue cracking were the two distress modes considered in this parametric analysis. Similar analyses can be conducted for other types of distresses (e.g., permanent deformation in unbound materials). The following factors were considered part of this evaluation:

- Pavement temperature.
- SHL-vehicle operating speed.
- Rehabilitation threshold.
- AADTT.
- Pavement structure.
- Reference-vehicle GVW.

4.1. INFLUENCE OF PAVEMENT TEMPERATURE

Pavement responses are highly sensitive to changes in climatic conditions, such as pavement temperature. Thus, the mechanistically based PDACs are expected to change with a change in pavement temperature. Figure 33 presents the variation in PDACs for AC permanent deformation and fatigue cracking as a function of *T*.

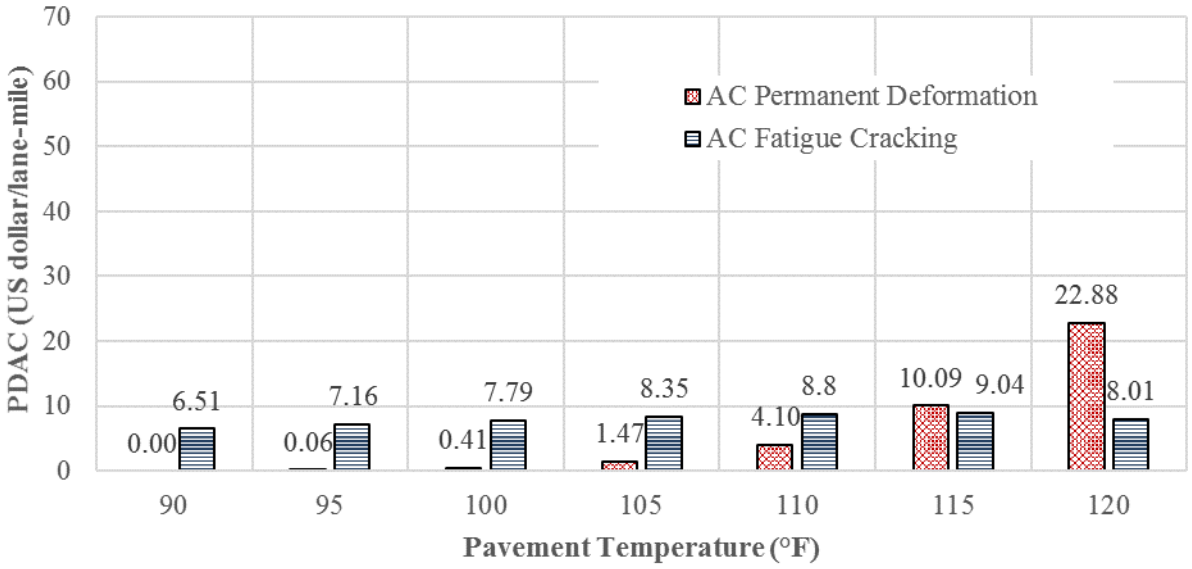

Figure 33. Graph. PDAC as a function of *T*.

The permanent deformation–based PDACs increased significantly with increasing temperatures. This result is mainly due to the decrease in AC-mixture stiffness at higher temperatures, leading

to greater PDACs. On the other hand, the relatively lower pavement damage induced by the SHL vehicle at lower temperatures resulted in lower PDACs. For instance, a permanent deformation–based PDAC of more than $22 per lane-mi was calculated when the SHL movement occurred when the pavement temperature was 120 °F. However, PDACs of the same SHL vehicle decreased to $0 when the pavement temperature was 90 °F or lower during the movement. A typical polymer-modified asphalt mixture from southern Nevada was used in this analysis.

The AC fatigue cracking–based PDACs were also determined. However, PDACs increased slightly with the increase in temperature up to 115 °F before decreasing at 120 °F. PDACs ranged between $6.51 and $9.04 per lane-mi. AC fatigue cracking–based PDAC was dominant at the lower temperatures, and the permanent deformation–based PDAC was dominant at the higher temperatures.

The implementation of different calibration constants in the estimation of pavement damage and subsequent PDAC might significantly alter the output results.

4.2. INFLUENCE OF SHL-VEHICLE OPERATING SPEED

Figure 34 presents the variation in PDACs as a function of vehicle operating speed. A notable change in PDACs is observed with the change in SHL-vehicle speed. An increase in PDACs was observed with the decrease in the SHL-vehicle operating speed. For instance, PDACs (based on both AC permanent deformation and fatigue) of more than $30 per lane-mi were calculated when the SHL vehicle was traveling at 5 mph. On the other hand, PDACs of $2.19 per lane-mi and $5.53 per lane-mi were calculated for the AC permanent deformation and AC fatigue cracking, respectively, when the SHL vehicle's operating speed was 60 mph.

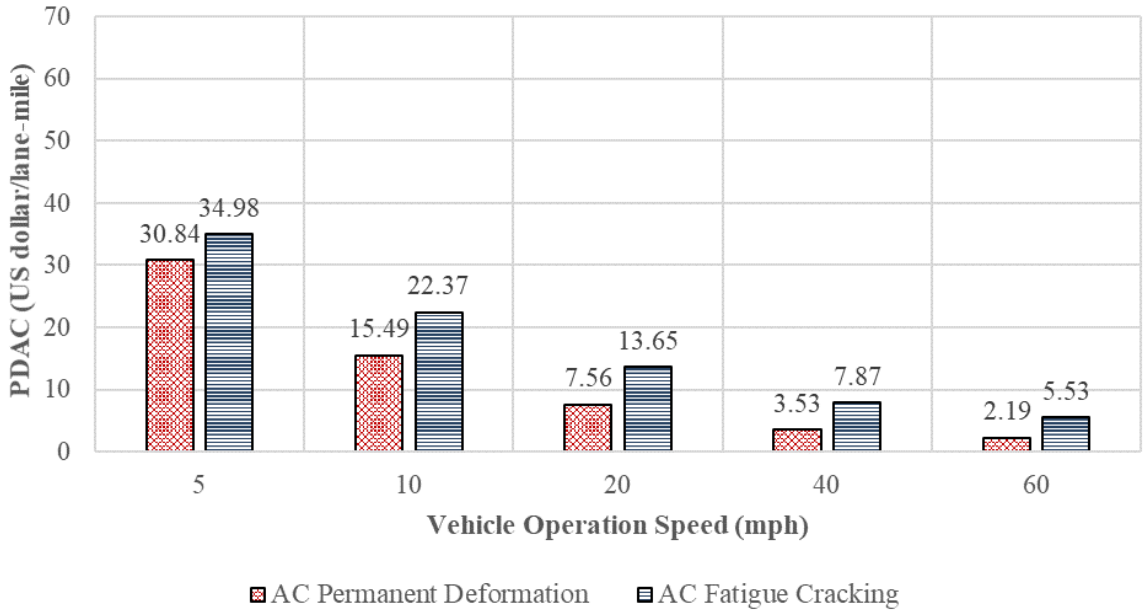

Figure 34. Graph. AC permanent deformation and AC fatigue cracking–based PDAC as a function of SHL-vehicle operating speed.

In summary, vehicle speed is an important factor that can significantly affect pavement damage and PDACs, mainly due to changes in the stiffness property of the asphalt mixture with the variation in vehicle speed, emphasizing the need for estimating pavement responses under moving SHL vehicles while accounting for the viscoelastic properties of the asphalt mixture.

It should be noted that SHL vehicles generally travel at lower speeds due to safety and operational considerations. Thus, SHAs and trucking companies should be aware of the higher risk for pavement damage and significantly higher PDACs when SHL vehicles travel at low speeds.

4.3. INFLUENCE OF REHABILITATION THRESHOLD

The rehabilitation threshold is an important factor that is used in the PDAC calculation. This value determines the required number of passes of both the SHL and reference vehicles to reach failure (section 3.1.2). As presented in figure 35 and figure 36, PDACs decrease significantly as the rehabilitation threshold increases. The reduction in PDACs is mainly due to a higher number of reference-vehicle passes required to reach failure. For instance, figure 35 shows that a PDAC of $13.88 per lane-mi is calculated when a failure criterion of 0.1 inch is considered for the AC permanent deformation. On the other hand, when the rehabilitation threshold increases to 0.3 inch, suggesting that more vehicle passes will be allowed on the pavement before a structural repair will be necessary, the value is reduced to $0.30 per lane-mi.

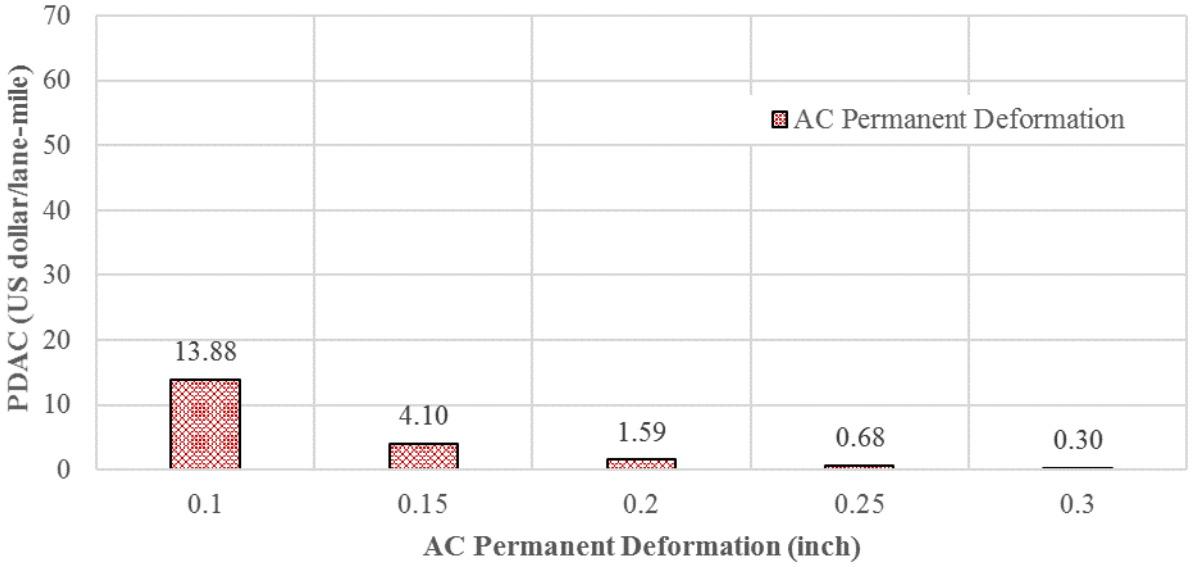

Figure 35. Graph. AC permanent deformation–based PDAC as a function of rehabilitation threshold.

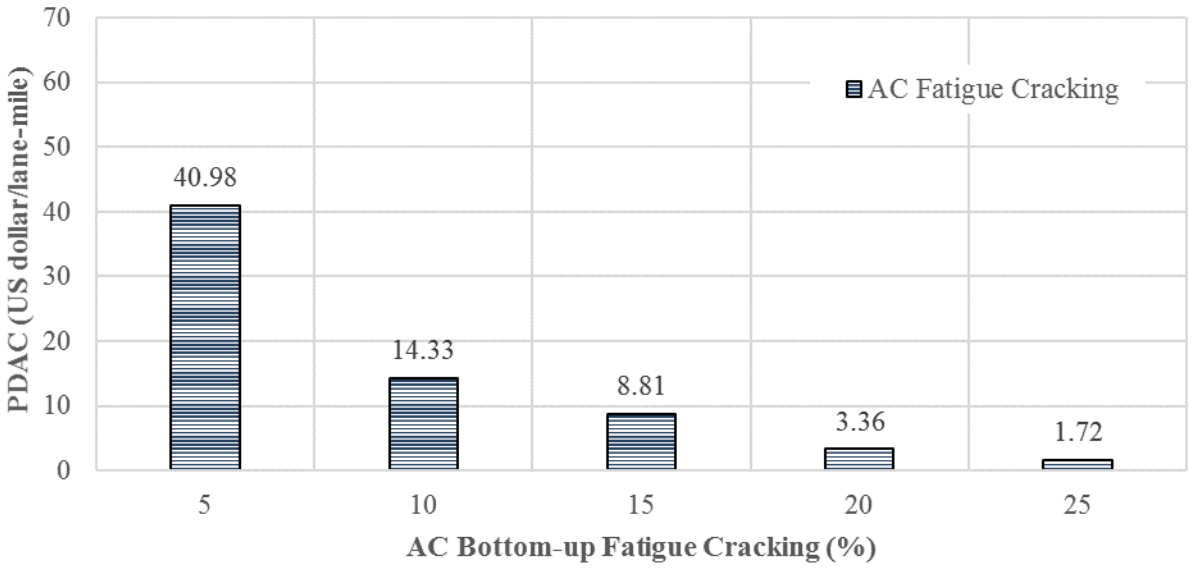

Figure 36. Graph. AC fatigue cracking–based PDAC as a function of rehabilitation threshold.

A similar behavior is presented in figure 36, where the AC fatigue cracking–based PDACs are presented. When the allowed percent in fatigue cracking area is increased to 25 percent, PDAC decreased from $40.98 (at 5 percent cracking) to $1.72 per lane-mi. Thus, lower PDACs are expected when an agency chooses to implement higher rehabilitation thresholds. The information presented in this section stresses the need for SHAs to select appropriate rehabilitation thresholds in PDAC calculations.

4.4. INFLUENCE OF AADTT

As presented in figure 37, a relatively small variation in PDACs is determined when implementing different AADTT values. For instance, when using an AADTT of 50, PDACs of $3.68 and $7.92 per lane-mi are calculated for AC permanent deformation and AC fatigue cracking, respectively. PDACs slightly increase when AADTT increases to 800. As presented in section 3.1.2, ADDTT is used to calculate the pavement section service life in years. The pavement service life value is subsequently used in the calculation of the *PWV* of the pavement-repair costs.

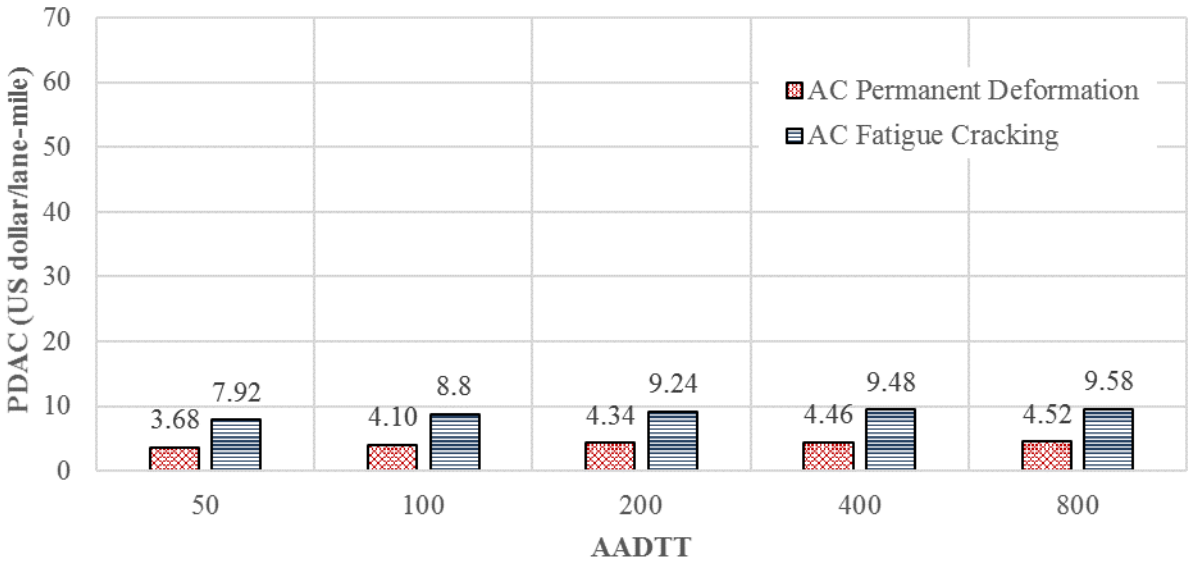

Figure 37. Graph. PDAC as a function of AADTT.

4.5. INFLUENCE OF PAVEMENT STRUCTURE

Figure 38 presents the variation in PDACs as a function of the pavement structure. For this example, the layer (e.g., AC, CAB) thicknesses were varied while maintaining the same material properties for the various layers as shown in table 4. It is clear that higher PDACs were calculated for pavement structures with lower structural capacity (e.g., lower AC-layer thickness and/or lower CAB-layer thickness). For instance, the highest AC permanent deformation–based PDAC was calculated for a pavement structure of 6 inches of AC over 6 inches of CAB. On the other hand, the permanent deformation–based PDAC was negligible for a pavement structure with 10 inches of AC over 10 inches of CAB. Similar findings were observed with PDACs calculated based on AC fatigue cracking.

In summary, greater damage is expected when SHL vehicles operate on pavement sections with a relatively low structural capacity. Thus, it is essential that SHAs be aware of the potential damage SHL vehicles could produce when operating on pavement sections with low structural capacity.

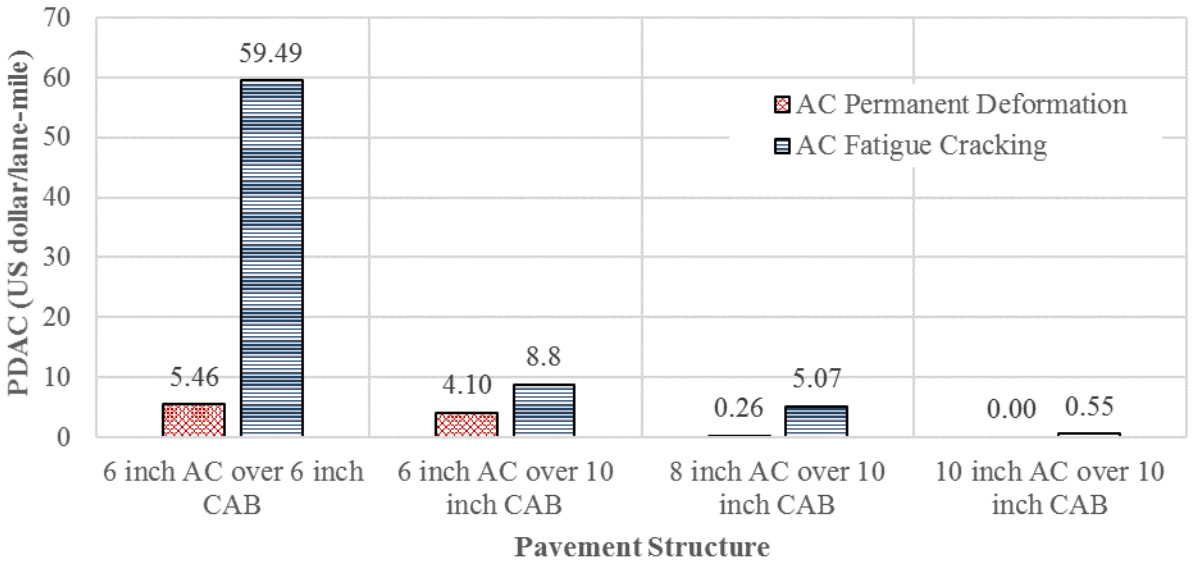

Figure 38. Graph. AC permanent deformation– and AC fatigue cracking–based PDAC as a function of pavement structure.

4.6. INFLUENCE OF REFERENCE-VEHICLE GVW

In previous examples, the reference vehicle was defined as a typical 18-wheel truck with a GVW of 80,000 lb with one steering axle of 12,000 lb and two tandem axles of 34,000 lb each. However, an SHA can select to use a different reference vehicle for the cost allocation analysis. Accordingly, five reference vehicles with different vehicle configurations were evaluated (table 10). The reference vehicles have GVWs ranging from 80,000 to 100,000 lb, and all have a single axle with single tires as the steering axle and a combination of tandem or tridem axles for the remaining axle groups. It should be noted that, whereas four of the evaluated reference vehicles had three axle groups, reference vehicle E consisted of four axle groups—one single-axle group as the steering axle and three tandem axle groups.

Table 10. Characteristics of the evaluated reference vehicles.

Reference-Vehicle Designation	GVW (lb)	Axle 1 Type	Axle 1 Load (lb)	Axle 2 Type	Axle 2 Load (lb)	Axle 3 Type	Axle 3 Load (lb)	Axle 4 Type	Axle 4 Load (lb)
A	80,000	Single	12,000	Tandem	34,000	Tandem	34,000	—	—
B	80,000	Single	12,000	Tridem	34,000	Tridem	34,000	—	—
C	90,000	Single	16,000	Tandem	37,000	Tandem	37,000	—	—
D	90,000	Single	16,000	Tridem	37,000	Tridem	37,000	—	—
E	100,000	Single	14,000	Tandem	28,667	Tandem	28,667	Tandem	28,667

—Not applicable.

As presented in figure 39, PDACs are slightly affected by the selection of the evaluated reference vehicles. A slight decrease in PDAC was observed when tridem axles (12 tires) were used instead of the respective tandem axles (8 tires). In summary, within the evaluated range for GVW and for the configurations examined, the selection of different reference vehicles had a minimal influence on the calculated PDACs.

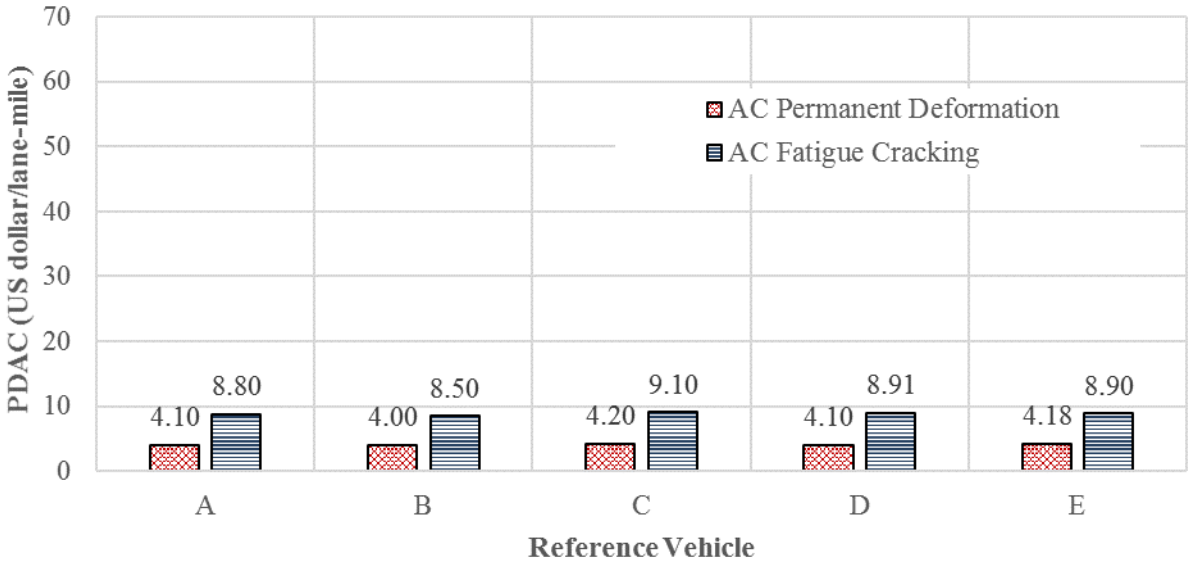

Figure 39. Graph. AC permanent deformation– and AC fatigue cracking–based PDAC for different reference vehicle.

4.7. SUMMARY

A parametric study was conducted to evaluate the influence of different factors on PDAC calculation. The evaluated factors included pavement temperature, SHL-vehicle operating speed, rehabilitation threshold, AADTT, pavement structure, and reference-vehicle selection. As presented in table 11, PDAC was found to be highly influenced by several of the evaluated factors. For instance, pavement temperature significantly affected the calculated PDACs. In fact, permanent deformation–based PDACs increased considerably with the increase in *T*. The SHL-vehicle speed also significantly affected PDACs. As vehicle speed decreased, PDACs increased significantly. PDACs were also highly influenced by the evaluated pavement structure and variation in rehabilitation threshold. High PDACs were determined for a pavement section with a low structural capacity and/or low rehabilitation thresholds.

Table 11. Impact level of factors evaluated in parametric study.

Factor	Potential Influence
Pavement temperature	High
SHL-vehicle operating speed	High
Rehabilitation threshold	High
AADTT	Low
Pavement structure	High
Reference-vehicle selection	Low

The research team also observed that PDACs are not as sensitive to AADTT and reference-vehicle selection (within the evaluated range) as other variables listed in table 11. In fact, slight changes in PDAC were determined as a function of AADTT variation. Similarly, the selection of the different reference vehicles in the PDAC analysis did not produce great variations in calculated PDACs.

Accordingly, since multiple factors are considered in the PDAC calculation, SHAs need to carefully select realistic and appropriate input values when determining PDACs from SHL-vehicle movements.

CHAPTER 5. OVERALL SUMMARY

Highway agencies issue permits to commercial vehicles exceeding established Federal weight limits. These permits are usually associated with a nominal fee sometimes ignoring the pavement damage caused by SHL movement. Recently, several studies have evaluated the impact of these vehicles on flexible pavements. These studies suggested cost allocation schemes correlating pavement damage and associated cost using different input parameters. In this report, an ME-based approach was proposed for the analysis of cost allocation associated with pavement damage under an SHL-vehicle movement. The approach considers different input parameters and provides a realistic methodology to assess pavement damage from a single pass of an SHL vehicle.

Prior to the determination of PDAC, ultimate failure analyses, buried utility risk analysis, and service limit failure analyses need to be conducted to assess the potential impact of SHL movement on flexible pavements. Mitigation strategies must be implemented whenever satisfactory results from these different analyses are not achieved. The various analyses required to assess the impact of an SHL-vehicle movement on the integrity of the pavement section are described in the other volumes of this series.[(1–9)] This report focuses on the cost allocation analysis, which is conducted only after all of the three aforementioned types of analyses are investigated and ruled out.

The presented approach employs input information that is commonly accessible to SHAs and implements an ME-based analysis that considers determining of critical pavement responses associated with different pavement distresses. Through a parametric analysis, it was found that several factors can influence the calculation of PDACs. Considering the information presented in this report, the following general observations can be made:

- PDACs are influenced by the input parameters of the cost allocation analysis. Consequently, SHAs should be prudent and exercise good judgment when quantifying the necessary input values for the analysis.

- PDACs are highly influenced by pavement temperature, SHL-vehicle operating speed, rehabilitation threshold value, and pavement structure.

- Because of the ME nature of the presented approach, the use of locally calibrated performance models is recommended in the estimation of PDACs.

REFERENCES

1. Hajj, E.Y., Siddharthan, R.V., Nabizadeh, H., Elfass, S., Nimeri, M., Kazemi, S.F., Batioja-Alvarez, D., and Piratheepan, M. (2018). *Analysis Procedures for Evaluating Superheavy Load Movement on Flexible Pavements, Volume I: Final Report*, Report No. FHWA-HRT-18-049, Federal Highway Administration, Washington, DC.

2. Nimeri, M., Nabizadeh, H., Hajj, E.Y., Siddharthan, R.V., Elfass, S., and Piratheepan, M. (2018). *Analysis Procedures for Evaluating Superheavy Load Movement on Flexible Pavements, Volume II: Appendix A, Experimental Program*, Report No. FHWA-HRT-18-050, Federal Highway Administration, Washington, DC.

3. Nimeri, M., Nabizadeh, H., Hajj, E.Y., Siddharthan, R.V., and Elfass, S. (2018). *Analysis Procedures for Evaluating Superheavy Load Movement on Flexible Pavements, Volume III: Appendix B, Superheavy Load Configurations and Nucleus of Analysis Vehicle*, Report No. FHWA-HRT-18-051, Federal Highway Administration, Washington, DC.

4. Nabizadeh, H., Hajj, E.Y., Siddharthan, R.V., and Elfass, S. (2018). *Analysis Procedures for Evaluating Superheavy Load Movement on Flexible Pavements, Volume IV: Appendix C, Material Characterization for Superheavy Load Movement Analysis*, Report No. FHWA-HRT-18-052, Federal Highway Administration, Washington, DC.

5. Nabizadeh, H., Hajj, E. Y., Siddharthan, R. V., Nimeri, M., Elfass, S., and Piratheepan, M. (2018). *Analysis Procedures for Evaluating Superheavy Load Movement on Flexible Pavements, Volume V: Appendix D, Estimation of Subgrade Shear Strength Parameters Using Falling Weigh Deflectometer*, Report No. FHWA-HRT-18-053, Federal Highway Administration, Washington, DC.

6. Nabizadeh, H., Nimeri, M., Hajj, E.Y., Siddharthan, R.V., Elfass, S., and Piratheepan, M. (2018). *Analysis Procedures for Evaluating Superheavy Load Movement on Flexible Pavements, Volume VI: Appendix E, Ultimate and Service Limit Analyses*, Report No. FHWA-HRT-18-054, Federal Highway Administration, Washington, DC.

7. Nabizadeh, H., Siddharthan, R.V., Elfass, S., and Hajj, E.Y. (2018). *Analysis Procedures for Evaluating Superheavy Load Movement on Flexible Pavements, Volume VII: Appendix F, Failure Analysis of Sloped Pavement Shoulders*, Report No. FHWA-HRT-18-055, Federal Highway Administration, Washington, DC.

8. Nabizadeh, H., Elfass, S., Hajj, E.Y., Siddharthan, R.V., Nimeri, M., and Piratheepan, M. (2018). *Analysis Procedures for Evaluating Superheavy Load Movement on Flexible Pavements, Volume VIII: Appendix G, Risk Analysis of Buried Utilities Under Superheavy Load Vehicle Movements*, Report No. FHWA-HRT-18-056, Federal Highway Administration, Washington, DC.

9. Kazemi, S.F., Nabizadeh, H., Nimeri, M., Batioja-Alvarez, D.D., Hajj, E.Y., Siddharthan, R.V., and Hand, A.J.T. (2018). *Analysis Procedures for Evaluating Superheavy Load Movement on Flexible Pavements, Volume X: Appendix I, Analysis Package for Superheavy Load Vehicle Movement on Flexible Pavement (SuperPACK)*, Report No. FHWA-HRT-18-058, Federal Highway Administration, Washington, DC.

10. National Cooperative Highway Research Program. (2008). *NCHRP Synthesis 378, State Highway Cost Allocation Studies: A Synthesis of Highway Practice*, Transportation Research Board, National Academy of Sciences, Washington, DC. Available online: http://www.trb.org/Publications/Blurbs/160297.aspx, last accessed October 30, 2018.

11. Federal Highway Administration. (2016). "Highway Cost Allocation Study." (website) Federal Highway Administration, Washington, DC. Available online: https:// www.fhwa.dot.gov/policy/otps/costallocation.cfm, last accessed May 1, 2014.

12. Federal Highway Administration. (2012). "Pavement Damage Analysis Tool (PaveDAT) for Overweight Truck Permit Calculation." (website) Federal Highway Administration, Washington, DC. Available online: https://www.fhwa.dot.gov/planning/freight_planning/talking_freight/june202012.cfm, last accessed October 30, 2018.

13. National Cooperative Highway Research Program. (2004). *Guide for Mechanistic-Empirical Design of New and Rehabilitated Pavement Structures*, National Cooperative Highway Research Program, Washington, DC. Available online: http://onlinepubs.trb.org/onlinepubs/archive/mepdg/home.htm, last accessed October 30, 2018.

14. Hajek, J.J., Tighe., S.L., and Hutchinson, B.G. (1998). "Allocation of Pavement Damage Due to Trucks Using a Marginal Cost Method." *Transportation Research Record, 1613*, pp. 50–60, Transportation Research Board, Washington, DC.

15. Ghaeli, R., Hutchinson, B.G., Hass, R., and Guillen, D. (2000). "Pavement and Bridge Cost Allocation Analysis of the Ontario, Canada, Intercity Highway Network." *Transportation Research Record, 1732*, pp. 99–107, Transportation Research Board, Washington, DC.

16. Boile, M., Ozbay, K., and Narayanan P. (2001). *Infrastructure Costs Attributable to Commercial Vehicles*, Report No. FHWA-NJ-2001-030, Federal Highway Administration, Washington, DC. Available online: https://cait.rutgers.edu/files/FHWA-NJ-2001-030.pdf, last accessed October 30, 2018.

17. Li, Z., Sinha, K., and McCarthy, P. (2001). "Methodology to Determine Load- and Non-Load-Related Shares of Highway Pavement Rehabilitation Expenditures." *Transportation Research Record, 1747*, pp. 79–88, Transportation Research Board, Washington, DC.

18. Straus, S.H., and Semmens, J. (2006). *Estimating the Cost of Overweight Vehicle Travel on Arizona Highways*, Report No. 528, Arizona Department of Transportation, Phoenix, AZ.

19. Fekpe, E. (2006). “Pavement Damage From Transit Buses and Motor Coaches.” Presented at the International Forum for Road Transport Technology, 9th International Symposium on Heavy Vehicle Weights and Dimensions (HWWD9), State College, PA.

20. Sadeghi, J.M., and Fathali, M. (2007). “Deterioration Analysis of Flexible Pavements Under Overweight Vehicles.” *Journal of Transportation Engineering, 133*(11), pp. 625–633, American Society of Civil Engineers, Reston, VA.

21. Hong, F., Prozzi, J.A., and Prozzi, J. (2007). “A New Approach for Allocating Highway Costs.” *The Journal of the Transportation Research Forum, 46*(2), pp. 5–19, Transportation Research Forum, Fargo, ND.

22. Timm, D.H., Turochy, R.E., and Peters, K.D. (2007). *Correlation Between Truck Weight, Highway Infrastructure Damage and Cost*, Report No. DTFH61-05-Q-00317, Auburn University Research Center, Auburn, AL.

23. Bai, Y., Schrock, S.D., Mulinazzi, T.E., Hou, W., Liu, C., and Firman, U. (2009). *Estimating Highway Pavement Damage Costs Attributed to Truck Traffic*, Kansas University Transportation Research Institute, Lawrence, KS. Available online: http://www2.ku.edu/~iri/publications/HighwayDamageCosts.pdf, last accessed October 30, 2018.

24. Tirado, C., Carrasco, C., Mares, J.M., Gharaibeh, N., Nazarian, S., and Bendana, J. (2010). “Process to Estimate Permit Costs for Movement of Heavy Trucks on Flexible Pavements.” *Transportation Research Record, 2154*, pp. 187–196, Transportation Research Board, Washington, DC.

25. Scott, J. and Ferrara, G.P. (2011). “Index for Estimating Road Vulnerability to Damage From Overweight Vehicles.” *Transportation Research Record, 2235*, pp. 1–8, Transportation Research Board, Washington, DC.

26. Hajek, J., Tighe, S., and Hutchinson, B. (1998). “Allocation of Pavement Damage Due to Trucks Using a Marginal Cost Method.” *Transportation Research Record, 1613*, pp. 50–56, Transportation Research Board, Washington, DC.

27. Prozzi, J., Murphy, M., Loftus-Otway, L., Banerjee, A., Kim, M., Wu, H., Prozzi, J.P., et al. (2012). *Oversize/Overweight Vehicle Permit Fee Study*, Report. No. FHWA/TX-13/0-6736-2, Federal Highway Administration, Washington, DC. Available online: http://ctr.utexas.edu/wp-content/uploads/pubs/0_6736_2.pdf, last accessed October 30, 2018.

28. Weissmann, A.J., Weissmann, J., Papagiannakis, A., and Kunisetty, J.L. (2012). “Potential Impacts of Longer and Heavier Vehicles on Texas Pavements.” *Journal of Transportation Engineering, 139*(1), pp. 75-80, American Society of Civil Engineers, Reston, VA.

29. Chowdhury, M., Putman, B., Pang, W., Dunning, A., Dey, K., and Chen L. (2013). *Rate of Deterioration of Bridges and Pavements as Affected by Trucks*, Report No. FHWA-SC-13-05, South Carolina Department of Transportation, Columbia, SC.

30. Chen, X., Lambert, J.R., Tsai, C. and Zhang, Z. (2013). “Evaluation of Superheavy Load Movement on Flexible Pavements.” *International Journal of Pavement Engineering*, *14*(5), pp. 440–448, Taylor & Francis, Abingdon, England.

31. Papagiannakis, A. (2015). *NCHRP Synthesis 476, Practices for Permitting Superheavy Load Movements on Highway Pavements*, Transportation Research Board, National Academy of Sciences, Washington, DC.

32. Hajj, E.Y., Batioja-Alvarez, D., and Siddharthan, R. (2016). “Assessment of Pavement Damage From Bus Rapid Transit: Case Study for State of Nevada.” *Transportation Research Record*, *2591*, pp. 70–79, Transportation Research Board, Washington, DC.

33. AASHTOWare® Pavement ME Design V2.3.1. Developed by American Association of State Highway and Transportation Officials, Washington, DC. Available online: http://me-design.com/MEDesign/, last accessed July 2, 2018.

34. Oh, J., Fernando, E., and Lytton, R. (2007). “Evaluation of Damage Potential for Pavements Due to Overweight Truck Traffic.” *Journal of Transportation Engineering*, *133*(5), pp. 308–317, American Society of Civil Engineers, Reston, VA.

35. Rada, G., Nazarian, S., Visintine, B., Siddharthan, R., and Thyagarajan, S. (2016). *Pavement Structural Evaluation at the Network Level*, Report No. FHWA-HRT-15-074, Federal Highway Administration, Washington, DC.

36. 3D-Move Analysis software V2.1. (2013). Developed by University of Nevada, Reno, NV. Available online: http://www.arc.unr.edu/Software.html#3DMove, last accessed September 19, 2017.

HRDI-20/12-18(WEB)E